IJP: Parasites and Wildlife 9 (2019) 159–173

Contents lists available at ScienceDirect

IJP: Parasites and Wildlife

journal homepage: www.elsevier.com/locate/ijppaw

Disentangling *Leucocytozoon* parasite diversity in the neotropics: Descriptions of two new species and shortcomings of molecular diagnostics for leucocytozoids

Ingrid A. Lotta[a,*], Gediminas Valkiūnas[b], M. Andreína Pacheco[c], Ananías A. Escalante[c], Sandra Rocío Hernández[a,d], Nubia E. Matta[a,**]

[a] Universidad Nacional de Colombia - Sede Bogotá- Facultad de Ciencias - Departamento de Biología - Grupo de Investigación Caracterización Genética e Inmunología, Carrera 30 No. 45-03, Bogotá, 111321, Colombia
[b] Institute of Ecology, Nature Research Centre, Akademijos 2, Vilnius-21, LT, 08412, Lithuania
[c] Institute for Genomics and Evolutionary Medicine (iGEM), Temple University, Philadelphia, PA, USA
[d] Red de Biología y Conservación de Vertebrados, Instituto de Ecología A.C., Xalapa, Veracruz, Mexico

ARTICLE INFO

Keywords:
Andean mountains
Birds
Co-infection
New species
Cotingidae
Grallaridae
Passeriforms

ABSTRACT

Avian communities from South America harbor an extraordinary diversity of *Leucocytozoon* species (Haemosporida, Leucocytozoidae). Here, of 890 birds sampled, 10 (1.2%) were infected with *Leucocytozoon* parasites. Among them, two new species were discovered and described. *Leucocytozoon grallariae* sp. nov. and *Leucocytozoon neotropicalis* sp. nov. were found in non-migratory highland passeriforms belonging to the Grallaridae and Cotingidae, respectively. They both possess gametocytes in fusiform host cells. However, due to combining microscopic examination and molecular detection, it was revealed that these parasites were present in co-infections with other *Leucocytozoon* species, which gametocytes develop in roundish host cells, therefore exhibiting two highly distant parasite lineages isolated from the same samples. Remarkably, the lineages obtained by cloning the mtDNA genomes were not captured by the classic nested PCR, which amplifies a short fragment of cytochrome *b* gene. Phylogenetic analyses revealed that the lineages obtained by the classic nested PCR clustered with parasites possessing gametocytes in roundish host cells, while the lineages obtained by the mtDNA genome PCR protocol were closely related to *Leucocytozoon* parasites possessing gametocytes in fusiform host cells. These findings suggest problems with the sensitivity of the molecular protocols commonly used to detect *Leucocytozoon* species. A detailed analysis of the primers used in the classic nested PCR revealed a match with DNA sequences from those parasites that possess gametocytes in roundish host cells (i.e., *Leucocytozoon fringillinarum*), while they differ with the orthologous regions in the mtDNA genomes isolated from the samples containing the two new species. Since these are mixed infections, none of the lineages detected in this study can be assigned accurately to the new *Leucocytozoon* morphospecies that develops in fusiform host cells. However, phylogenetic analyses allowed us to hypothesize their most probable associations. This study highlights the need for developing detection methods to assess the diversity of *Leucocytozoon* parasites accurately.

1. Introduction

The Andes in South America are recognized as hotspots for avian endemism. This region includes approximately 133 different ecosystems (Morrone, 2001; Josse et al., 2009) with more than 2000 avian species reported, including nearly 600 endemic species (Myers et al., 2000; Herzog and Kattan, 2011). Such host species richness seems to drive a high diversity of avian haemosporidian parasites that is just starting to be characterized using microscopy and Polymerase Chain Reaction (PCR)-based detection methods (i.e. Merino et al., 2008; Rodríguez et al., 2009; Jones et al., 2013; Mantilla et al., 2013, 2016; Matta et al., 2014; Galen and Witt, 2014; Harrigan et al., 2014; González et al., 2014, 2015; Marzal et al., 2015; Lotta et al., 2016; Moens et al., 2016; Moens and Pérez-Tris, 2016; Cadena-Ortiz et al.,

* Corresponding author. Universidad Nacional de Colombia - Sede Bogotá- Facultad de Ciencias - Departamento de Biología - Grupo de Investigación Caracterización Genética e Inmunología, Carrera 30 No. 45-03, Bogotá, 111321, Colombia.
** Corresponding author.
E-mail addresses: ialottaa@unal.edu.co (I.A. Lotta), nemattac@unal.edu.co (N.E. Matta).

https://doi.org/10.1016/j.ijppaw.2019.05.002
Received 30 January 2019; Received in revised form 7 May 2019; Accepted 7 May 2019

2018; de Aguilar et al., 2018; Gil-Vargas and Sedano-Cruz, 2019).

Molecular techniques present significant advantages for parasite detection, particularly in samples with very low parasitemia (sub-microscopic infections). Many molecular protocols targeting to different molecular markers such as the rRNA (Richard et al., 2002), nuclear sequences (Bensch et al., 2004), the apicoplast (Caseinolytic protease C-Clpc) (Martinsen et al., 2008), and mitochondrial genes (Cytochrome b -*cytb*, Cytochrome oxidase subunit I and III – *cox1, cox3*) (Escalante et al., 1998; Bensch et al., 2000; Perkins and Schall, 2002; Hellgren et al., 2004; Pacheco et al., 2018b) have been used with diagnosis purpose. Currently, most of the avian haemosporidian inventories rely mainly on molecular detection. Unfortunately, most of the sequences of haemosporidian, including *Leucocytozoon,* reported in the Neotropics remain without being associated with a morphospecies because few studies applied both microscopic and molecular diagnosis in parallel. That is an obstacle for a reliable estimate of parasite species diversity.

PCR-based methods commonly overlook the presence of co-infections (Bernotienė et al., 2016; Pacheco et al., 2018a). The two main reasons are 1) the primers may have a higher affinity for one of the parasites in the sample, and 2) there may be an uneven amount of the template for each of the species or lineages in the co-infected samples (Perez-Tris and Bensch, 2005; Bernotienė et al., 2016; Pacheco et al., 2018a). Nevertheless, there are many reported cases where the amplification fails to detect haemosporidian parasite DNA in samples with an evident high intensity of parasitemia (Zehtindjiev et al., 2012; Schaer et al., 2015; Bernotienė et al., 2016), indicating that other variables are also involved in the PCR performance in co-infections (Pacheco et al., 2018a). Indeed, co-infections of avian haemoporasites are common in natural populations (Perez-Tris and Bensch, 2005; Van Rooyen et al., 2013; Bernotienė et al., 2016; Pacheco et al., 2018a), making this problem far more complicated (Bernotienė et al., 2016; Ciloglu et al., 2018; Pacheco et al., 2018a). Although recent publications have provided alternatives to overcome the issue of mixed infections (Perez-Tris and Bensch, 2005; Bernotienė et al., 2016; Pacheco et al., 2018a), the molecular detection of lineages belonging to the same genus in the same sample and their linkage to certain morphospecies remains challenging. For example, in the case of birds sampled in Colombian mountain ranges, co-infections of *Leucocytozoon* species with parasites of other genera have been detected in 25.4% of samples. Furthermore, in 18.2% of the co-infections two or more species of *Leucocytozoon* were observed in the same blood film (Lotta et al., 2016).

In this study, new leucocytozoid species were found in two non-migratory species of passerines (Undulated Antpitta, *Grallaria squamigera* and Green and black Fruiteater, *Pipreola riefferii*) from highland ecosystems of Colombia. These parasites were described using both microscopic and molecular diagnosis. Importantly, both bird species were co-infected with different lineages of *Leucocytozoon* species. Using morphological and phylogenetic analyses, a possible linkage was proposed between the new morphospecies under description and other lineages amplified from co-infections. Furthermore, we also discussed current problems in molecular diagnosis of *Leucocytozoon* parasites.

2. Materials and methods

2.1. Study sites

During this study, 840 birds belonging to 139 species were caught using mist nets in the central and eastern Andean mountain ranges of Colombia (Table 1). In the central mountain chain (*Cordillera Central*), 686 birds belonging to 118 species were captured during April, July, August, and December of 2015 and January of 2016 (Table 1). Sample sites included three distinct life zones (Cuatrecasas, 1958): (i) Sub-andean Forest (SF) (1800–2600 m above sea level (masl)); represented by the Fauna and Flora Sanctuary *Otún Quimbaya* (FFS), *El Cedral* station and *Ucumarí* Natural Regional Park (NRP); (ii) the Andean Forest (AF) (2900–3500 masl) as found in the locality of *El Bosque*, and (iii) the

Table 1
Birds captured in *Los Nevados* National Natural Park, and *Palacio* forest at *Chingaza* NNP in this study.

	Life zone	Altitudinal range	N° cap (N° infected) per chain of mountains	
			Eastern	Central
Anseriformes				
Anatidae				
Anas flavirostris	AF	2900–3500	1(0)	
Apodiformes				
Trochilidae				
Adelomyia melanogenys	SAF	1800–2600		5(0)
Aglaiocercus kingii	SAF	1800–2600		1(0)
Amazilia franciae	SAF	1800–2600		4(0)
Boissonneaua flavescens	AF	2900–3500		1(0)
Boissonneaua flavescens	SAF	1800–2600		2(0)
Coeligena	SAF	1800–2600		7(0)
Coeligena helianthea	AF	2900–3500	1(0)	
Coeligena torquata	SAF	1800–2600		3(0)
Coeligena torquata	AF	2900–3500		1(0)
Colibri coruscans	AF	2900–3500		3(0)
Colibri thalassinus	SAF	1800–2600		3(0)
Doryfera ludovicae	SAF	1800–2600		2(0)
Ensifera	AF	2900–3500	1(0)	3(0)
Eriocnemis cupreoventris	AF	2900–3500	2(0)	
Eriocnemis derbyi	AF	2900–3500		14(0)
Eriocnemis derbyi	SAF	1800–2600		1(0)
Heliangelus amethysticollis	AF	2900–3500	1(0)	
Heliangelus exortis	AF	2900–3500	1(0)	7(0)
Heliangelus exortis	SAF	1800–2600		5(1)
Lafresnaya lafresnayi	AF	2900–3500	6(0)	4(0)
Metallura tyrianthina	AF	2900–3500		3(0)
Metallura tyrianthina	P	3900–4100		2(0)
Phaethornis guy	SAF	1800–2600		4(0)
Phaethornis syrmatophorus	SAF	1800–2600		3(0)
Schistes geoffroyi	SAF	1800–2600		1(0)
Columbiformes				
Columbidae				
Zenaida auriculata	SAF	1800–2600		2(0)
Charadriiformes				
Charadiidae				
Vanellus chilensis	SAF	1800–2600		2(0)
Falconiformes				
Accipitridae				
Rupornis magnirostris	SAF	1800–2600		1(0)
Passeriformes				
Cinclidae				
Cinclus leucocephalus	AF	2900–3500	3(0)	
Corvidae				
Cyanolyca viridicyanus	SAF	1800–2600		2(0)
Cyanocorax yncas	SAF	1800–2600		3(0)
Cotingidae				
Pipreola riefferii[§]	AF	2900–3500		1(1)
Dendrocolaptidae				
Pseudocolaptes boissonneautii	AF	2900–3500	1(0)	
Emberizidae				
Arremon brunneinucha	SAF	1800–2600		4(0)
Arremon brunneinucha	AF	2900–3500	2(1)	
Arremon torquatus	AF	2900–3500	4(0)	
Atlapetes albinucha	SAF	1800–2600		6(0)
Atlapetes albinucha	AF	2900–3500	2(0)	
Atlapetes pallidinucha	AF	2900–3500	7(1)	
Atlapetes schistaceus	AF	2900–3500	6(1)	
Zonotrichia capensis	SAF	1800–2600		93(0)
Zonotrichia capensis	P	3900–4100		6(0)

(*continued on next page*)

Table 1 (*continued*)

	Life zone	Altitudinal range	N° cap (N° infected) per chain of mountains	
			Eastern	Central
Zonotrichia capensis	AF	2900–3500	17(0)	30(0)
Fringillidae				
Astragalinus psaltria	AF	2900–3500		2(0)
Astragalinus psaltria	SAF	1800–2600		4(0)
Euphonia laniirostris	SAF	1800–2600		3(0)
Euphonia xanthogaster	SAF	1800–2600		4(0)
Saltator atripennis	SAF	1800–2600		1(0)
Furnariidae				
Cinclodes excelsior	P	3900–4100		6(0)
Dendrocincla tyrannina	AF	2900–3500		1(0)
Dendrocincla tyrannina	SAF	1800–2600		2(0)
Hellmayrea gularis	AF	2900–3500	1(0)	
Leptasthenura andicola	P	3900–4100		6(0)
Lepidocolaptes lacrymiger	SAF	1800–2600		1(0)
Margarornis squamiger	AF	2900–3500	12(0)	
Premnoplex brunnescens	AF	2900–3500		1(0)
Premnoplex brunnescens	SAF	1800–2600		2(0)
Synallaxis azarae	SAF	1800–2600		10(0)
Syndactyla subalaris	SAF	1800–2600		1(0)
Xiphocolaptes promeropirhynchus	SAF	1800–2600		3(0)
Grallariidae				
*Grallaria squamigera**	AF	2900–3500	1(1)	
Hirundinidae				
Orochelidon murina	AF	2900–3500	2(0)	7(0)
Orochelidon murina	P	3900–4100		5(0)
Pygochelidon cyanoleuca	SAF	1800–2600		14(0)
Pyroderus scutatus	SAF	1800–2600		4(0)
Stelgidopteryx ruficollis	SAF	1800–2600		2(0)
Icteridae				
Molothrus bonariensis	SAF	1800–2600		2(0)
Momotidae				
Momotus momota	SAF	1800–2600		1(0)
Parulidae				
Basileuterus tristriatus	SAF	1800–2600		2(0)
Cardellina canadiensis	SAF	1800–2600		8(1)
Myioborus sp.	AF	2900–3500	1(0)	
Myioborus miniatus	SAF	1800–2600		6(0)
Myioborus ornatus	AF	2900–3500	4(0)	6(0)
Myiothlypis coronata	AF	2900–3500		1(0)
Myiothlypis coronata	SAF	1800–2600		5(0)
Myiothlypis nigrocristatus	AF	2900–3500	13(0)	1(0)
Setophaga fusca	SAF	1800–2600		1(0)
Rhinocryptidae				
Scytalopus infasciatus	AF	2900–3500	1(0)	
Scytalopus micropterus	AF	2900–3500	2(0)	
Thraupidae				
Anisognathus igniventris	AF	2900–3500	3(0)	
Anisognathus lacrymosus	AF	2900–3500		5(0)
Buthraupis montana	AF	2900–3500		1(1)
Catamblyrhynchus diadema	AF	2900–3500	3(0)	
Catamenia homochroa	P	3900–4100		12(0)
Catamenia inornata	P	3900–4100		18(0)
Conirostrum rufum	AF	2900–3500	1(0)	
Diglossa albilatera	AF	2900–3500	2(0)	3(0)
Diglossa albilatera	SAF	1800–2600		1(0)
Diglossa cyanea	AF	2900–3500	7(0)	18(0)
Diglossa cyanea	SAF	1800–2600		3(0)
Diglossa humeralis	P	3900–4100		9(0)
Diglossa humeralis	AF	2900–3500		11(0)
Diglossa sittoides	SAF	1800–2600		6(0)
Euphonia laniirostris	SAF	1800–2600		3(0)
Euphonia xanthogaster	SAF	1800–2600		4(0)
Hemispingus atropileus	AF	2900–3500	4(0)	2(0)
Hemispingus frontalis	AF	2900–3500		1(0)
Hemispingus sp.	AF	2900–3500		1(0)
Hemispingus superciliaris	SAF	1800–2600		1(1)
Hemispingus superciliaris	AF	2900–3500	3(0)	1(0)
Hemispingus verticalis	AF	2900–3500	1(0)	
Phrygilus unicolor	P	3900–4100		64(0)
Pipraeidea melanonota	SAF	1800–2600		5(0)
Saltator atripennis	SAF	1800–2600		3(0)
Saltator maximus	SAF	1800–2600		1(0)
Sericossypha albocristata	SAF	1800–2600		5(0)
Sporophila nigricollis	SAF	1800–2600		14(0)
Tangara arthus	SAF	1800–2600		1(0)
Tangara cyanicollis	SAF	1800–2600		1(0)
Tangara gyrola	SAF	1800–2600		2(0)
Tangara heinei	SAF	1800–2600		1(0)
Tangara labradorides	SAF	1800–2600		1(0)
Tangara nigroviridis	SAF	1800–2600		2(0)
Tangara vassorii	AF	2900–3500		6(1)
Tangara vitriolina	SAF	1800–2600		6(0)
Thraupis episcopus	SAF	1800–2600		4(0)
Thraupis palmarum	SAF	1800–2600		2(0)
Tiaris olivaceus	SAF	1800–2600		2(0)
Troglodytidae				
Henicorhina leucophrys	SAF	1800–2600		7(0)
Henicorhina leucophrys	AF	2900–3500	3(0)	
Pheugopedius genibarbis	SAF	1800–2600		3(0)
Pheugopedius mystacalis	SAF	1800–2600		3(0)
Troglodytes aedon	P	3900–4100		2(0)
Troglodytes aedon	AF	2900–3500		2(0)
Troglodytes aedon	SAF	1800–2600		8(0)
Troglodytes solstitialis	SAF	1800–2600		1(0)
Turdidae				
Catharus aurantiirostris	SAF	1800–2600		1(0)
Catharus ustulatus	SAF	1800–2600		1(0)
Myadestes ralloides	SAF	1800–2600		1(0)
Turdus fuscater	P	3900–4100	2(0)	2(0)
Turdus fuscater	AF	2900–3500		5(0)
Turdus fuscater	SAF	1800–2600		1(0)
Turdus ignobilis	SAF	1800–2600		14(0)
Tyrannidae				
Contopus fumigatus	SAF	1800–2600		1(0)
Elaenia albiceps	SAF	1800–2600		1(0)
Elaenia frantzii	SAF	1800–2600		1(0)
Empidonax alnorum	SAF	1800–2600		1(0)
Empidonax sp.	SAF	1800–2600		1(0)
Mecocerculus leucophrys	AF	2900–3500	3(0)	7(0)
Mecocerculus leucophrys	SAF	1800–2600		1(0)
Mecocerculus stictopterus	AF	2900–3500	12(0)	
Mionectes olivaceus	SAF	1800–2600		1(0)
Mionectes striaticolis	SAF	1800–2600		11(0)
Mionectes srtiaticolis	AF	2900–3500	2(0)	
Myiarchus tuberculifer	SAF	1800–2600		1(0)
Myiophobus sp.	SAF	1800–2600		1(0)
Myiotheretes striaticollis	AF	2900–3500	1(0)	
Nephelomyias pulcher	SAF	1800–2600		1(0)
Ochthoeca cinnamomeiventris	AF	2900–3500	3(0)	3(0)
Ochthoeca diadema	SAF	1800–2600		2(0)
Ochthoeca diadema	AF	2900–3500	4(0)	
Ochthoeca fumicolor	P	3900–4100		5(0)
Ochthoeca rufipectoralis	AF	2900–3500		1(0)

(*continued on next page*)

Table 1 (*continued*)

	Life zone	Altitudinal range	N° cap (N° infected) per chain of mountains	
			Eastern	Central
Phyllomyias nigrocapillus	SAF	1800–2600		1(0)
Phyllomyias nigrocapillus	AF	2900–3500	1(0)	
Phylloscartes poecilotis	SAF	1800–2600		2(0)
Pyrrhomyias cinnamomeus	SAF	1800–2600		4(0)
Sayornis nigricans	SAF	1800–2600		9(0)
Serpophaga cinerea	SAF	1800–2600		4(0)
Sicalis flaveola	SAF	1800–2600		3(0)
Tyrannus melancholicus	SAF	1800–2600		2(0)
Uromyias agilis	AF	2900–3500	6(0)	
Uromyias agilis	SAF	1800–2600		1(0)
Zimmerius viridiflavus	SAF	1800–2600		12(0)
Vireonidae				
Cyclarhis nigrirostris	SAF	1800–2600		1(0)
Piciformes				
Ramphastidae				
Aulacorhynchus haematopygus	SAF	1800–2600		1(0)
Picidae				
Picumnus olivaceus	SAF	1800–2600		1(0)
Trogoniformes				
Trogonidae				
Trogon collaris	SAF	1800–2600		1(0)
Trogon personatus	AF	2900–3500		1(0)
Total per locality			154(4)	686(6)
Leucocytozoon sp. prevalence			2.6%	0.9%
Leucocytozoon sp. nov. prevalence			0.6%	0.14%
Leucocytozoon sp. overall prevalence				1.19%
Total				840(10)

The number of birds capture per species followed of the occurrence of *Leucocytozoon* sp. (in parenthesis), is given. [§]Hosts infected with *L. neotropicalis* sp. nov, * hosts infected with *L. grallariae* sp. nov. Life zone as follow Sub-Andean Forest (SAF); Andenan Forest (AF); Paramo (P); and altitudinal range data is also provided.

Paramo ecosystem (P) (3900–4100 masl) as represented by the *Otún* Lake. In the eastern mountain range (*Cordillera Oriental*) 154 birds, belonging to 42 species were captured during January of 2015 and December 2016 (Table 1) at the *Bosque Palacio de Chingaza* (NNP), which is an Andean Forest (2900–3500 masl) life zone.

2.2. Sampling and blood film examination

Birds were identified according to the taxonomic lists of the South American Classification Committee (SACC) (Remsen et al., 2012). Blood samples were collected by brachial or tarsal vein puncture or toenail clipping (last method for the tiny hummingbirds). For each bird, three thin smears were made, and 50 µl of blood were stored in an EDTA-anticoagulant solution or SET buffer (0.05 M Tris, 0.15 M NaCl, 0.5 M EDTA, pH 8.0). Blood films were air dried immediately in the field, and then fixed with absolute methanol and stained with 30% Giemsa solution in the laboratory according to Valkiūnas (2005). The smears were double-blind scanned by microscopic examination using an Olympus BX43 microscope, and digital images were captured with an Olympus DP27 digital camera, processed with cellSens software standard 1.13 (Olympus, Tokyo, Japan). For the morphological characterization of parasites, more than 100 images were taken, and the best images for morphometrical measurements were selected using ImageJ (Schneider et al., 2012), following the recommendations of Valkiūnas et al. (2010). The intensity of parasitemia was determined by an actual counting of the number of infected cells per 10,000 erythrocytes (Muñoz et al., 1999). A Student's t-test implemented in XLSTAT (Addinsoft, 2017) was used to determine statistical significance between the mean values of parasite morphometric measurements. A *P*-value of 0.05 or less was considered significant.

2.3. DNA extraction, PCR amplification and sequencing of cytochrome b gene and DNA mitochondrial genome

DNA extractions were carried out using a standard phenol–chloroform protocol (Sambrook et al., 1989). Cytochrome b gene (*cytb*) amplifications were done by using a nested PCR protocol (Hellgren et al., 2004). Purifications of PCR products were performed with ethanol and ammonium acetate protocol according to Bensch et al. (2000) and then visualized on a 1.5% agarose gel. All purified PCR products were subsequently sequenced in both senses using a 3730xl DNA Analyzer (Applied Biosystems, Foster City, CA, USA). Five independent amplifications were carried out for all available samples infected with the new *Leucocytozoon* species and made careful visual inspection of the electropherograms to confirm that the lineage sequences obtained were not chimeric products as a result of mixed infections. The *cytb* sequences obtained in this study were submitted to GenBank under accession numbers MH909275 (L_GRSQU_02) and MH909276 (L_PIRIE_02).

In addition to the *cytb* gene, two *Leucocytozoon* mitochondrial genomes (mtDNA) from one Undulated Antpitta (*Grallaria squamigera,* Grallaridae) and one Green-and-black Fruiteater (*Pipreola riefferii*, Cotingidae) were amplified, cloned and sequenced. PCR products were amplified with TaKaRa LA TaqTM Polymerase (TaKaRa Mirus Bio Inc., Shiga, Japan) as described by (Pacheco et al., 2011, 2018b) using primers forward 5′ GA GGA TTC TCT CCA CAC TTC AAT TCG TAC TTC and reverse 5′ CAG GAA AAT WAT AGA CCG AAC CTT GGA CTC. Then, a nested PCR was performed using the internal oligos forward 5′ TTT CATCCTTAAATCTCGTAAC 3′/reverse 5′ GACCGAACCTTGGACTCTT 3'. PCR amplifications for both PCR (outer and inner) were carried out in a 50 µl volume using 20 ng of total genomic DNA. The PCR conditions were as follow: a partial denaturation at 94 °C for 1 min and 30 cycles of 30 s at 94 °C and 7 min at 68 °C, followed by a final extension of 10 min at 72 °C. Following the manufacturer's directions, six independent PCR products (bands of approximately 6 kb) were excised from the gel, purified using QIAquick® Gel extraction kit (Qiagen, GmbH, Hilden, Germany), and four of them were cloned in the pGEM®-T Easy Vector systems (Promega, Madison, WI, USA) and two were directly sequenced. For at least three clones from each independent PCR and two PCR products, we sequenced both strands using an Applied Biosystems 3730 capillary sequencer. There were no inconsistencies among the clones and between the direct sequencing of the PCR products and clones. We submitted the mtDNA genome sequences to GenBank under accession numbers MK103894 and MK103895. In addition, following the above-mentioned methodologies, new DNA extractions and amplifications of the parasite *cytb* gene were performed using samples infected with *Leucocytozoon pterotenuis* (Blood film: GERPH07966- Blood sample: UNAL:GERPH:PA262), and a *Leucocytozoon* sp. (Blood film: GERPH-07737- Blood sample:UNAL:GERPH:AN18). These two parasites were previously detected and described by us in other species of the Grallariidae (*Grallaria ruficapilla* and *Grallaria quitensis* respectively; as *Leucocytozoon pteroteunis* (Lotta et al., 2015).

2.3.1. Phylogenetic analysis

First, phylogenetic relationships of the new *Leucocytozoon* species were estimated from an alignment using partial *cytb* gene sequences (476 base pairs (bp)). This alignment, constructed in MEGA 7 (Kumar et al., 2016) and aligned with Clustal Omega tool (McWilliam et al., 2013), included 88 lineages of parasites from passerine and non-passerine of South American birds and lineages belonging to unidentified morphospecies that had been deposited in the GenBank (Benson et al., 2015) and MalAvi database (Bensch et al., 2009), as well as the new

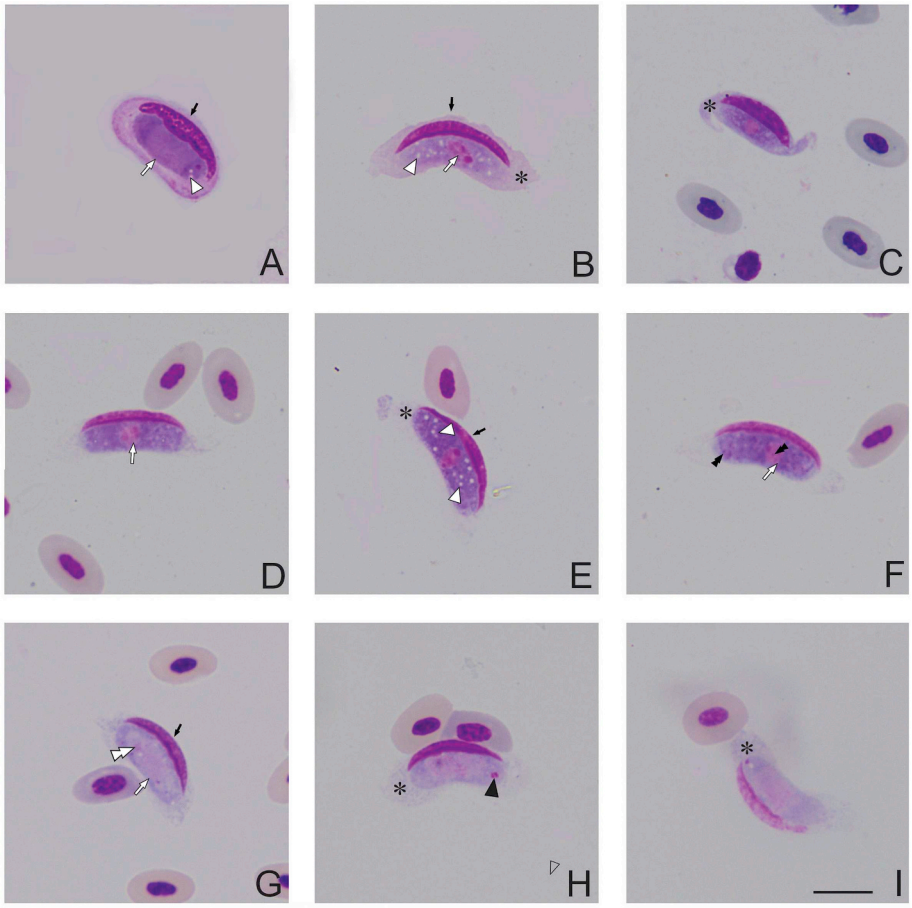

Fig. 1. *Leucocytozoon grallariae* sp. nov. from Undulated Antpitta (*Grallaria squamigera*) captured at Palacio forest in the Chingaza National Natural Park (NNP), Colombia. Immature gametocytes (A–C), macrogametocytes (D–F) and microgametocytes (G–I) in fusiform host cells. Nucleus of host cells (*black arrows* ⬆) possessing mature gametocytes assumes a slender waning moon shape (D–I). Parasite nuclei are indicated by white arrows (⇧) and parasite nucleolus – by *double white arrow tips* (⇧). Host cell cytoplasm is distorted by developing parasites forming a thin rim that develops into the cytoplasmic processes (*asterisk* *). In mature gametocytes, vacuoles are indicated by *white arrow tips* (◁). Volutin granules are indicated by *double black arrow tips* (➘) and azurophilic granule by *black arrow tips* (▲). Giemsa-stained thin blood films. Scale bar = 10 μm.

sequences reported in this study (Supplementary Table S1). A second alignment was done with only 28 *cytb* partial sequences (476 bp) including the partial *cytb* sequences available and the *cytb* from the mtDNA genomes obtained in this study. Finally, an alignment was done using 26 mtDNA genomes (5487 bp excluding gaps) in order to show the phylogenetic relationship between the new parasites that we found, and the ones reported previously. It is important to note that for both birds infected with the new *Leucocytozoon* sp., no inconsistencies between the mtDNA genomes clones and mtDNA genomes obtained by direct sequencing of PCR products were found.

In all the cases we performed phylogenetic reconstructions using Bayesian methods implemented on MrBayes v3.1.2 (Ronquist and Huelsenbeck, 2003), through the CIPRES portal (Miller et al., 2010). For partial *cytb* sequences and mtDNA genomes, phylogenetic relationships were estimated under the General Time-Reversible model (GTR + Γ + I), which was the best model that fit these data, according to the corrected Akaike information criterion implemented on jModelTest 2.1.1 (Darriba et al., 2012). Two independent Markov Chain Monte Carlo (MCMC) simulations were conducted simultaneously for 5×10^6 generations, sampled every 100 generations. After discarding 25% of the trees as a burn-in period, a majority rule consensus phylogeny was obtained from 75,000 trees. Then, the phylogeny was visualized and edited using FigTree v1.3.1 (Rambaut, 2006). We estimated genetic distances between lineages using a Kimura two-parameter model of substitution, implemented in MEGA 7.0 (Kumar et al., 2016).

2.4. Analysis of primers

Affinity of the primers proposed by Hellgren et al. (2004) with the *cytb* gene sequences obtained from *Leucocytozoon* parasites was evaluated by aligning the oligonucleotides with lineages of parasite species with gametocytes developing in roundish host cells, like *Leucocytozoon fringillinarum* and *L. dubreuili* (Perkins, 2008; Pacheco et al., 2018b) and lineages obtained from those parasites, which gametocytes develop in fusiform host cells, such as *L. pterotenuis* (Lotta et al., 2015) and the two species described in this study.

2.5. Ethical statement

Samples were collected using a non-invasive methodology, approved by the "*Comité de Bioetica of Departamento de Ciencias para la Salud Animal," Facultad de Medicina Veterinaria y de Zootecnia, Universidad Nacional de Colombia* (Permit number CBE-FMVZ-016). Bird capture and manipulation were done in a way that reduced stress caused by these activities. Once the blood samples were taken, the birds were released. Fieldwork were conducted under authorization of "*Unidad Administrativa Especial del Sistema de Parques Nacionales Naturales de Colombia UAESPNN - Subdirección técnica*" and "*Autoridad Nacional de Licencias Ambientales, ANLA*" (file 4120E183893 of 2011, resolution 0787 of 2013, and resolution 255 of 2014).

3. Results

3.1. Prevalence of infection and description of parasites

Leucocytozoon infections were detected in 10 birds of the 840 sampled (1.2%) by microscopic examination of blood smears. Molecular characterization was made only on the positive samples by microscopic examinations. Whilst gametocytes of *Leucocytozoon quynzae*, *L fringillinarum* and *Leucocytozoon* sp. were observed in eight individuals belonging to Emberizidae, Parulidae, Thraupidae and Trochilidae (Table 1), two new morphologically readily distinct species of

Leucocytozoon were found in widely distributed South American native non-migrating passerine bird species (McMullan et al., 2011; BirdLife International, 2017a, 2017b): one Undulated Antpitta (*Grallaria squamigera*) and one Green and black Fruiteater (*Pipreola riefferii*) (Table 1).

Undulated Antpitta (Grallaridae) is distributed in the Andean mountain ranges above 2000 masl in Neotropical humid forests and scrublands of Bolivia, Peru, Ecuador, Colombia and Venezuela (BirdLife International, 2017a). In general, Antpitta birds are elusive, rarely seen and demanding in their capture and sampling. Green and black Fruiteaters (Cotingidae) are arboreal birds that inhabit tropical moist montane forests above 1000 to 3300 masl from Peru to Venezuela (BirdLife International, 2017b).

3.2. Description of parasites

3.2.1. Leucocytozoon (Leucocytozoon) grallariae sp. nov

Young gametocytes (Fig. 1) markedly influence the shape of host cells from earliest stages of their development. Growing parasites were of oval or ellipsoid shapes; they closely adhered to the host cell nuclei, which were markedly enlarged, deformed and assumed crescent shapes (Fig. 1A–C). The host cell cytoplasm was present around growing gametocytes, and it was very evident. Advanced young gametocytes often possessed invaginations on their sides, which were opposite to the host cell nuclei, and that gave the growing gametocytes the shapes of giant beans with approximately equally rounded ends (Fig. 1 B). Host cells assumed ellipsoid shapes from early stages of gametocyte development (Fig. 1 A).

Macrogametocytes developed in fusiform host cells (Fig. 1). In *Leucocytozoon* species, as the gametocytes develop, they cause considerable distortion of the host cells, producing two distinct host cell-parasite complex forms: roundish and fusiform. In this *Leucocytozoon* species, the gametocytes only in fusiform host cells were observed. Gametocytes induced marked hypertrophy and deformation of the host cells and displacement of their nuclei, which lay on the periphery of gametocytes. The host cell nuclei acquired slender waning moon shapes; usually extending up to ½ of the circumference of gametocytes, and they could reach the fusiform processers, but they never extended into the processes (Fig. 1C–E). In both types of host cells, the nuclei looked homogenous.

The host-cell cytoplasm forms two short cytoplasmic processes located close to ends of gametocytes. Fusiform processes were variable in form (Fig.1 D, F–I) nevertheless, those processes, which length was similar to their largest width were common (Table 2), and that was a characteristic feature of the development of this species. It is worth mentioning that the cytoplasmic processes were occasionally observed as being unequally long at both sides of the same parasite (Fig. 1H and I), probably as a consequence of the host cell deformation during blood film preparation. Some remnants of host cell cytoplasm were seen covering around half of the perimeter of the gametocyte-host cell complex as a thin rim (Fig. 1G–I), which is uncommon in avian leucocytozoids. Additionally, host cells with fully grown gametocytes could possess irregular shapes and blunt processes, while they were often pointed in host cells with immature growing gametocytes (Fig. 1G–I).

The gametocyte cytoplasm was granular in appearance; it often possessed small vacuoles and tiny volutin granules (Fig. 1E and F). Vacuoles were of different sizes, but not greater than 3.0 μm in their maximum diameter; they were observed in 97 gametocytes. Vacuoles were seen in growing (immature) gametocytes (Fig. 1 B). Parasite nuclei were compact; they were seen mainly in the central position (67% of reported cases) in gametocytes and were of roundish (Fig. 1D–F) or various oval (Fig. 1 E) shapes. Nucleoli were visible in 50% of the gametocytes.

The general configuration of the **Microgametocytes** and other features (Fig. 1G–I) were as for macrogametocytes with the usual haemosporidian sexual dimorphic characters that were the pale stained cytoplasm and large diffuse nuclei (Table 2). The proportion of microgametocytes and macrogametocytes in the type material was approximately 3:5. A prominent azurophilic granule was seen only in the cytoplasm of 90% of microgametocytes (Fig. 1H and I) located close to the parasite nuclei.

Table 2
Morphometric parameters of gametocytes and host cells of *Leucocytozoon grallariae* sp. nov.

Feature	*Leucocytozoon grallariae* sp. nov	
	Macrogametocyte n = 15	Microgametocyte n = 10
Parasite		
Length	14.7–23.6 (20.2 ± 2.5)	15.8–21.3 (18.5 ± 2.1)
Width	4,5-5,5 (5,4 ± 0,5)	4.1–6.1 (5.1 ± 0.6)
Area	79.7–109.0 (97.4 ± 9.6)	71.3–93.4 (81.7 ± 6.0)
Perimeter	39.9–54.4 (47.1 ± 4.3)	39.6–49.3 (43.5 ± 3.4)
Parasite nucleus		
Length	2.7–4.9 (3.6 ± 0.6)	7.2–12.9 (10.0 ± 1.9)
Width	3.1–5.4 (4.4 ± 0.6)	3.0–4.5 (3,7 ± 0.4)
Area	9.9–18.0 (13.1 ± 2.2)	23.4–49.4 (32.8 ± 9.0)
Host-cell parasite complex		
Length	24.8–32.1 (29.6 ± 2.5)	24.7–33.9 (29.4 ± 2.7)
Width	7.3–10.3 (8.5 ± 1.0)	7.0–10.3 (8.4 ± 0.9)
Area	162.6–196.4 (185.1 ± 12.8)	152.2–188.1 (168.8 ± 11.0)
Host-cell nucleus		
Length	15.8–22.9 (21.1 ± 1.8)	17.5–21.6 (18.9 ± 1.2)
Width	1.5–3.6 (2.2 ± 0.5)	2.0–2.6 (2.3 ± 0.2)
Area	27.0–49.1 (32.6 ± 5.5)	25.7–34.8 (31.3 ± 2.3)
Perimeter of parasite covered	15.3–22.1 (21.1 ± 1.8)	17.2–20.5 (18.2 ± 1.1)
Cytoplasmic processes[a]		
Length	3.3–7.6 (5.0 ± 1.0)	3.8–7.8 (5.5 ± 1.3)
Width	3.7–8.0 (5.7 ± 1.0)	4.4–8.0 (5.8 ± 1.1)
Area	15.4–35.3 (24.1 ± 3.7)	20.0–35.3 (26.4 ± 4.5)

[a] Measurements are given in μm or μm^2 (for area). Minimum and maximum values as well as mean ± SD are provided.

[a] Only one of 2 cytoplasmic processes was measured for each parasite.

3.2.2. Taxonomic summary

Type host: Undulated Antpitta *Grallaria squamigera* (Grallaridae, Passeriformes).

Additional hosts: unknown.

Type locality: Palacio Forest at the transition zone of Chingaza NNP (4° 41′ N, 73° 50′ W, 2950 masl), Cundinamarca, Colombia.

Distribution: This parasite has been recorded only at the type locality.

Type specimens: Hapantotype (accession No. UNAL:GERPH:PA340 -XI, intensity of parasitemia 0.25%, collected by Nubia E. Matta, 18 January 2015) and deposited in the biological collection GERPH (Grupo de Estudio Relación Parásito Hospedero) at the Universidad Nacional de Colombia, Bogotá, Colombia. Parahapantotypes (accession Nos., UNAL:GERPH:PA340 – I to UNAL:GERPH:PA340 –X and UNAL:GERPH:PA340 –XII to UNAL:GERPH:PA340 -XIX) are deposited in the same collection. Digital images of blood stages of the parasite in the type preparations are available on request from GERPH.

DNA sequences: The partial mitochondrial DNA genome (5891 bp) that includes *cox1*, *cox3* and *cytb* genes (GenBank accession number MK103895) was obtained from the type host *Grallaria squamigera.*

Site of infection: Blood cells, of which the origin is unclear due to marked deformation caused by gametocytes.

Prevalence: Only one individual of the host species was collected and found to be infected, so the sample size does not allow to estimate of prevalence. The parasite was morphologically detected in 1 of out of 684 examined birds (0.12%). This or similar parasites were not found in 840 sampled birds of different species at Palacio Forest and Los Nevados NNP (Table 1).

Etymology: The species name refers to the host genus name *Grallaria,*

which is the type host of the parasite belongs.

3.2.3. Remarks

Seventeen species of *Leucocytozoon*, which gametocytes develop in fusiform host cells are reported to date (Supplentary Table S2), but only four of them, *Leucocytozoon maccluri* (Greiner, 1976), *Leucocytozoon balmorali* (Peirce, 1984), *Leucocytozoon hamiltoni* (Valkiūnas et al., 2002), and *Leucocytozoon pterotenuis* (Lotta et al., 2015) are described in birds of the.

Passeriformes. The new species described here, *Leucocytozoon grallariae,* found in a passerine bird, can be readily distinguished from the four *Leucocytozoon* species mentioned above due to two distinctive morphological characters. First, the fusiform processes are short (Table 2) in the host cells with fully grown gametocytes of *L. grallariae* (Fig. 1D–I). The length of these processes often does not exceed their largest width (Table 2, Fig. 1 G, H). This is not the case in *L. maccluri, L. balmorali, L. hamiltoni* and *L. pterotenuis*; their gametocytes develop fusiform host cells, which fusiform processes are greater in length than in largest width. Second, the host cell nuclei assume the slender waning moon shapes, and the nuclei could reach the cytoplasmic processes, but never extended into them. None of these two characters are features of *L. maccluri, L. balmorali, L. hamiltoni, L. pterotenuis* (see Valkiūnas, 2005; Lotta et al., 2015).

Gametocytes in many *Leucocytozoon* species described in non-passerine birds develop in fusiform host cells (Table S2). During *L. grallariae* infection, the host cell nuclei extend up to ½ of the circumference of the gametocytes, and the host cell nuclei might reach the beginning of cytoplasmic processes. This feature is not characteristic of other leucocytozoids where gametocytes developed fusiform host cells, and this feature can be used during identification of *L. grallariae.*

During microscopic examination of the type material, a co-infection with *Leucocytozoon* species with gametocytes developing in roundish host cells were detected (Fig. 3, Table S3). Gametocytes developing in fusiform host cells were ten times more often observed (parasitemia intensity is 0.25%) than gametocytes developing in roundish host cells (0.01%). In addition to the lineage associated with the GenBank No. MK103895 for the partial mtDNA genome reported above, one *cytb* lineage of 476 bp (L_GRSQU 02 GenBank No. MH909275) was amplified from the same blood sample of this type host. Genetic distance between both lineages was 0.23 (Table 5), which suggest that they belong to a different species. However, from these two lineages obtained in the same sample, we propose that lineage MK103895 obtained by cloning corresponds to the parasite, which gametocytes develop in fusiform host cells in the sample (see discussion below).

3.2.4. Leucocytozoon (Leucocytozoon) neotropicalis sp. nov

Macrogametocytes (Fig. 2A–E) develop in fusiform host cells; the shape of gametocytes is oval-elongate (their length is greater than width, Table 3). However, the morphology of host-parasite complexes with fusiform processes is readily distinguishable from *L. grallariae* (compare Fig. 1 F, H and Fig. 2 A, F, I). The host cell nuclei are pushed aside, deformed like a homogeneous band of variable width that extends close to half of the circumference of gametocyte (Fig. 2 A, I), but never extends into the cytoplasmic processes. This is similar in both *L. grallariae* and *L. neotropicalis* cells, so these parasites cannot be distinguished by this character (see the description of *L. grallariae* and compare Fig. 2 D, F, H and Fig. 2 A, G, I.). These species can be readily distinguished due to the length of the cytoplasmic processes. Mainly, the latter is significantly longer (Student's t-test, $\alpha = 0.05$ $P < 0.0001$) and narrower in their maximum width ($P < 0.0001$) than in *L. grallariae* (see Table 2, compare Fig. 2. F, H and Fig. 2 A, F, I).

Two long thin fusiform spindle-shaped processes of the host cells' cytoplasm reach up to 14 μm (Table 3), and that never is observed in *L. grallariae*. The length of the cytoplasmic processes can be different in the same host-parasite complex (Fig. 2J and K), and that probably is a result of deformation during the preparation of blood films. Cytoplasmic processes are thin and often flattened appearing like a ribbon (Fig. 3F–H). It is important to note that mature gametocytes often have a flattened form on the side, located on the opposite side of the host cell nuclei (Fig. 2 H, J-K). This character is not observed in *L. grallariae* (Fig. 1I–K).

In the type material, we observed tiny volutin granules and small vacuoles (up to 0.47 μm in diameter) in 47.9% of fully grown gametocytes (Fig. 2A–E). The parasite nucleus was roundish in 49.3% of 103 observed gametocytes (Fig. 2A–C) or elongated (Fig. 2 E); its position was mainly more or less central, but sometimes was off-centre. The nucleolus was variable both in shape and position, being visible in 53.2% of 103 observed parasites (Fig. 2 B, D).

Microgametocytes (Fig. 2F–I): General configuration and other features were similar to the macrogametocytes with the usual haemosporidian sexual dimorphic characters. The proportion of microgametocytes and macrogametocytes in the type material was approximately 1:2.

Taxonomic summary.

Type host: Green-and-black Fruiteater *Pipreola riefferii* (Cotingidae, Passeriformes).

Additional hosts: unknown.

Type locality: El Bosque, Los Nevados National Natural Park (NNP) (4° 43 N; 75° 27 W, 3150 masl), Risaralda, Colombia.

Type specimens: Hapantotype (accession Nos. UNAL:GERPH:OT1354-II). The intensity of the infection of the lineage MK103894 is 0.33%, it was collected by Melisa Galarza (27 December 2015) and deposited in the biological collection GERPH (Grupo de Estudio Relación Parásito Hospedero) at the Universidad Nacional de Colombia, Bogotá, Colombia. Parahapantotypes (accession Nos. UNAL:GERPH:OT1354-I, UNAL:GERPH:OT1354-III, other data as for the hapantotype) are deposited in the same collection. Digital images of the blood stages of the parasite in the type preparations are available on request from GERPH.

Partial mitochondrial DNA genome (5811 bp) that includes *cox1*, *cox3* and *cytb* genes (GenBank accession number MK103895) was obtained from the type host *Pipreola riefferii*.

Site of infection: Blood cells, the specific cell is unknown due to the marked deformation by developing gametocytes.

Prevalence: Only one individual of the host species was collected and found infected, so the sample size does not allow to estimate the prevalence. Parasite was detected by microscopy in 1 of out of 684 examined birds (0.12%). In the type locality, 1 of 686 birds captured at Los Nevados NNP (0.14%) was infected, as determined by microscopic examination.

Etymology: The species name (*neotropicalis*) was derived from the name of the zoogeographical region where this parasite was found.

3.2.5. Remarks

Leucocytozoon neotropicalis is one of the six *Leucocytozoon* species that parasitize passerine birds and possess gametocytes developing in fusiform host cells. The main differences between *L. neotropicalis* and *L. grallariae* are specified in the description of the former parasite. Both of these new leucocytozoids have gametocytes developing fusiform host cells, which can be distinguished from other leucocytozoids due to the unique shape of their host cell nuclei (see Remarks on *L. grallariae*).

Due to the presence of long and narrow cytoplasmic processes in host cells, *L. neotropicalis* is similar to *L. lovati* (Valkiūnas, 2005) and *L. eurystomi* (Bennett et al., 1993; Valkiūnas, 2005) (Table 3). However, the nuclei of host cells never reach the cytoplasmic processes in the last two parasites. Because of this character, these species can be readily distinguished.

Microscopic examination of blood smears from type series revealed the presence of co-infection of a parasite with gametocytes developing in roundish host cells. Overall, the configuration of the nuclei in roundish host cells resembles the same characters observed in the *L. fringillinarum* group (Fig. 3.). The reported gametocytes in roundish host

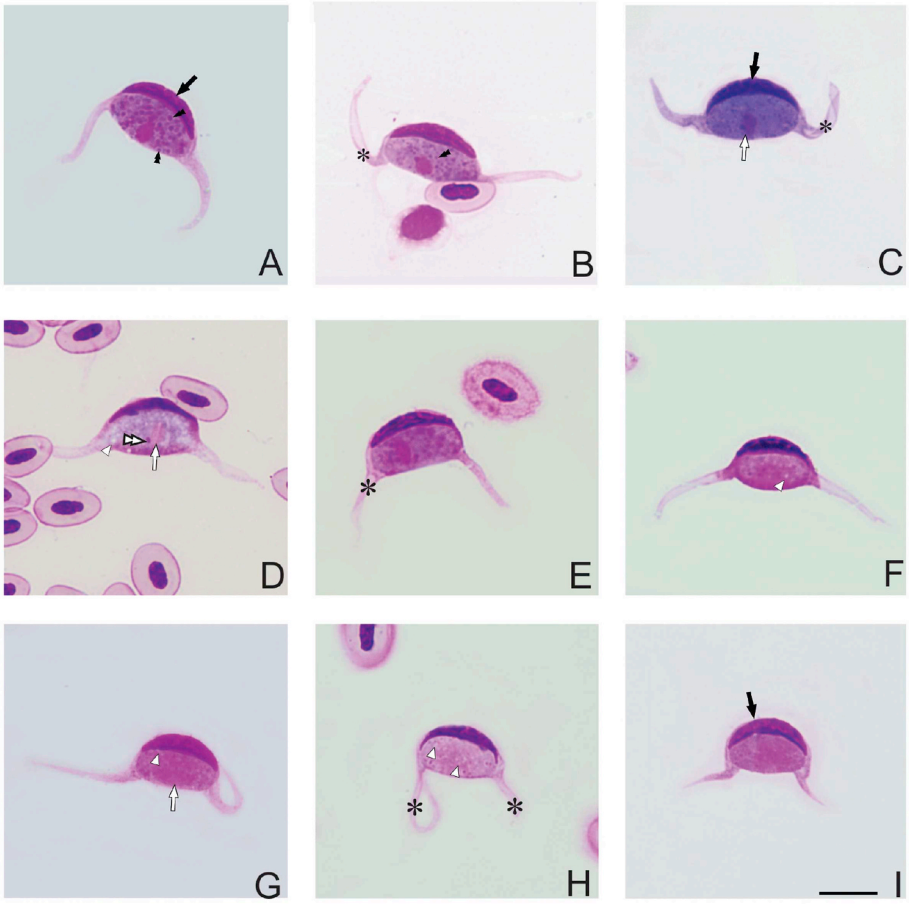

Fig. 2. *Leucocytozoon neotropicalis* sp. nov. from the peripheral blood of its type vertebrate host Green-and-black Fruiteater (*Pipreola riefferii*) captured at Los Nevados NNP, Colombia. Macrogametocytes (A–E) and microgametocytes (F–I). *Black arrows* (⬆) indicate the deformed host cell nuclei. Parasite nuclei are indicated by *white arrow* (⇧) and nucleoli are shown by *double white arrowtips* (⇗). Volutin granules are indicated by *double black arrowtips* (⬊) and vacuoles – by *white arrowtips* (◁). Uneven cytoplasmic processes may acquire a ribbon-like appearance (*asterisk* *). Giemsa-stained thin blood films. Scale bar = 10 μm. (For interpretation of the references to color in this figure legend, the reader is referred to the Web version of this article.)

cells are bigger than those observed in the sample with coinfection with *L. grallariae* (Student's t-test for parasite area: $p < 0.0001$, $\alpha = 0.05$, Table S3). In contrast to the macrogametocytes of *L. neotropicalis*, the volutin granules are not pronounced or absent in roundish gametocytes of this parasite (Fig. 3D–F). It worth mentioning that, for both new species as well as for *L. pterotenuis* (Lotta et al., 2015), the gametocytes developing in fusiform host cells were the most common, and their parasitemia was on average ten to seventeen times higher than the species with gametocytes developing roundish host cells. Indeed, in the type material of *L. neotropicalis* parasitemia of gametocytes developing fusiform host cells was 0.21%, while it did not exceed 0.01% for gametocytes developing roundish host cells.

Two distantly related lineages with a genetic distance of 0.29 between them (L_PIRIEF_01, *cytb* gene GenBank No. MH909276 and

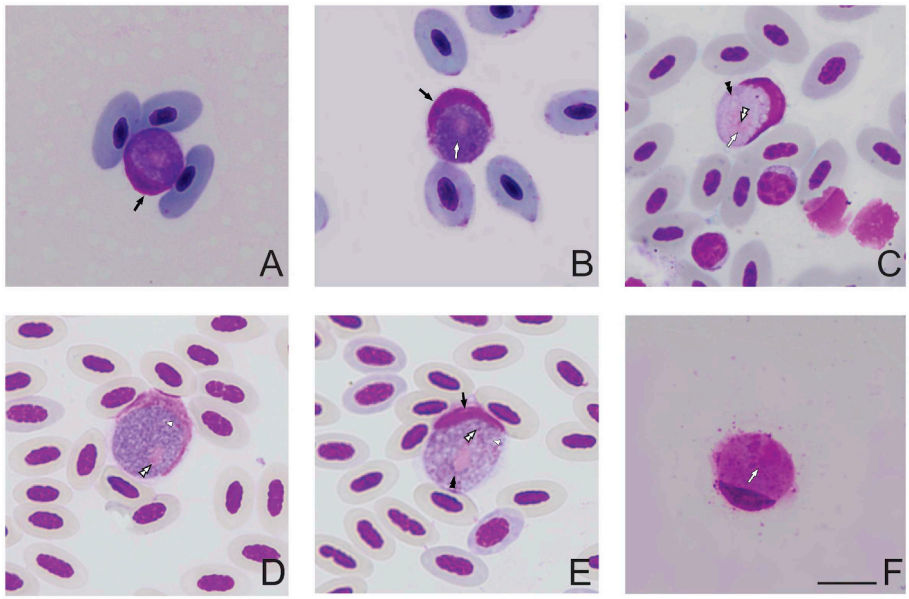

Fig. 3. Gametocytes developing roundish host cells observed in type material of *Leucocytozoon grallariae* (A–C) and *Leucocytozoon neotropicalis* (D–F). Host cell nucleus (black arrows ⬆) deformed as a cap resembles the parasites of the *Leucocytozoon fringillinarum* group. The white arrow indicates the parasite nuclei (⇧), double white arrow tips shows the nucleolus (⇗). Vacuoles (*white arrow tips* ◁) are present, while volutin granules *(double black arrow tips* ⬊) are few or absent in some gametocytes. Giemsa-stained thin blood films. Although gametocytes in roundish host cells were observed in both samples, those co-existing with *Leucocytozoon grallariae* (A–C), are significative smaller than *Leucocytozoon* sp. gametocytes found in type host of *L. neotropicalis* (D–F) (see Table S3). Scale bar = 10 μm.

Table 3
Morphometric parameters of gametocytes and host cells of *Leucocytozoon neotropicalis* sp. nov. Measurements of *Leucocytozoon eurystomi* and *Leucocytozoon lovati* are provided for comparison. Measurements are given in μm or μm^2 (for area). Minimum and maximum values as well as mean ± SD are provided.

Feature	*Leucocytozoon neotropicalis* sp. nov		*Leucocytozoon eurystomi*[a,b]	*Leucocytozoon lovati*[b]
	Macrogametocyte n = 6	Microgametocyte n = 1		
Parasite				
Length	14.4–16.0 (15.3 ± 0.6)	11.4–17.9 (13.6 ± 1.5)	22.6–29.6 (25.2 ± 1.3)	14.1–22.0 (17.5 ± 1.4)
Width	7.0–8.2 (7.8 ± 1.0)	5.7–10.0 (7.8 ± 1.4)	7.0–12.2 (8.1 ± 1.0)	6.7–13.1 (11.0 ± 0.7)
Area	86.1–101.2 (95.2 ± 4.9)	64.9–114.9 (83.7 ± 17.4)	(182 ± 18.5)	
Perimeter	34.1–40.9 (38.8 ± 1.6)	31.4–48.9 (37.4 ± 4.8)	(63.0 ± 5.9)	
Parasite nucleus				
Length	2.0–3.1 (2.8 ± 0.5)	5.3–10.5 (8.0 ± 1.5)	2.8–6.4 (4.1 ± 0.4)	3.2–6.8 (4.2 ± 0.3)
Width	3.3–4.1 (4.0 ± 0.4)	4.4–7.0 (5.6 ± 0.8)	1.4–5.7 (3.5 ± 0.3)	1.8–4.4 (3.6 ± 0.3)
Area	7.0–9.6 (8.6 ± 1.0)	32.5–48.4 (41.4 ± 4.7)	(11.8 ± 2.6)	
Host-cell parasite complex				
Length	35.5–56.6 (44.7 ± 5.3)	29.8–55.8 (41.4 ± 8.6)	(39.2 ± 6.3)	
Width	9.5–10,8 (10.2 ± 0.5)	9.2–10.8 (9.9 ± 0.5)	(9.1 ± 0.7)	
Area	161.0–200.1 (181.8 ± 10.4)	127.4–181.7 (151.2 ± 13.0)	(202.2 ± 21.1)	
Host-cell nucleus				
Length	14.8–19.7 (17.7 ± 1.8)	14.2–18.3 (16.3 ± 1.3)	18.3–26.0 (21.7 ± 2.3)	9.8–16.3 (13.5 ± 1.5)
Width	2.4–3.7 (2.9 ± 3.0)	2.4–3.7 (3.0 ± 0.4)		
Area	28.2–39.6 (35.7 ± 4.3)	23.6–42.0 (33.6 ± 5.3)	(39.0 ± 7.2)	
Perimeter of parasite covered	14.1–18.2 (16.5 ± 1.8)	14.2–18.3 (16.3 ± 1.3)	(16.9 ± 2.3)	
Cytoplasmic processes[c]				
Length	11.3–22.0 (15.7 ± 2.8)	7.6–24.4 (14.8 ± 4.5)		
Width	2.6–5.4 (3.8 ± 0.8)	1.9–5.3 (3.7 ± 0.9)		
Area	18.2–29.0 (25.0 ± 5.3)	14.4–26.1 (21.2 ± 3.2)		

[a] According to Bennet et al., (1993).
[b] According to Valkiūnas (2005).
[c] Only one of 2 cytoplasmic processes was measured for each parasite.

partial mtDNA genome that included *cytb*, *cox1*, *cox3,* GenBank No. MK103894), were amplified from the same sample, which makes it difficult to link the lineages with their morphotypes. Based on phylogenetic analysis, we suggest that the last one lineage (GenBank No. MK103894) corresponds to *L neotropicalis* n. sp. (see discussion below).

3.3. Sequencing of the cytochrome b gene and the DNA mitochondrial genome

Two lineages were isolated from each of the samples containing *L. grallariae* or *L. neotropicalis*. The partial *cytb* fragments obtained using the primers suggested by Hellgren et al. (2004) were very distant from the *cytb* lineages obtained by the mtDNA genome amplification protocol (Pacheco et al., 2011, 2018). In other words, different *Leucocytozoon* parasite sequences were obtained in the same sample using different protocols and that corresponded to the microscopic observation of possible co-infections in these samples.

Even though both protocols for the amplification of *cytb* fragments and the mtDNA genome were run at least two times independently, each protocol amplified different lineages (lineages isolated from *G. squamigera:* GenBank *cytb* accession No. MH909275 vs GenBank mtDNA accession No. MK103895; lineages isolated from *P. riefferii:* GenBank *cytb* accession No. MH909276 vs GenBank mtDNA accession No. MK103894). Similar results were obtained when new molecular studies were performed with the Grallaridae bird samples reported by Lotta et al. (2015), where parasites were described as *Leucocytozoon pterotenuis.* With the new analysis, we realized that the *cytb* fragment obtained along with the partial mitochondrial genomes (mtDNA) identified with GenBank accession No. KM272250 and the short *cytb* fragment amplified with Hellgren's primers identified with GenBank accession No. KY646032 were different. Thereby, we will be referring to the description of *Leucocytozoon pteroteunuis* (Lotta et al., 2015) as a partial description of the parasite (according to the (International Commission on Zoological Nomenclature, 1999) the description "in part"), because according to the molecular analyses performed, gametocytes in roundish host cells observed in the sample likely do not belong to *L. pterotenuis*, but to other *Leucocytozoon* species (see discussion). Thus, the species name *L. pterotenuis* is valid only in part, mainly for gametocytes developing in fusiform host cells, but not to gametocytes in roundish host cells.

3.4. Analysis of primer affinities

The success of amplification is highly dependent on the primer's affinity for the target sequence and the parasitemia that determines the amount of parasite present DNA (Perez-Tris and Bensch, 2005; Pacheco et al., 2018a). After verification of affinities of the primers proposed by Hellgren et al. (2004) with the all complete *cytb* gene sequences of *Leucocytozoon* parasites available for passerine birds, it was noticed that oligo-sequences matched the *cytb* sequences of *L. fringillinarum* (Genbank accession No. KY653765) and *L. dubreuili* (Genbank accession No. KY653795), which both have gametocytes developing roundish host cells (Fig. 4 A, B). In contrast, we noticed that the primer HaemR2L did not completely match with the mtDNA sequences obtained using the mtDNA genome amplification protocol used for *L. pterotenuis* (in part) (Genbank No.KM610046). Indeed, the base pairs at the 3′ end of the primer, as well as the two last base pair of the 5', did not match with the *cytb* gene sequences obtained from the mtDNA genome of *L. grallariae* (Genbank No. MK103895) nor *L. neotropicalis* (Genbank No. MK103894) (Fig. 4).

3.5. Phylogenetic analysis

In the phylogenetic reconstructions based on partial mitochondrial genomes and 476 *cytb* fragments (Fig. 5 and S1), two main clades that resemble the classification of parasites according to morphological features were observed. Thus, parasite lineages of leucocytozoids with gametocytes developing round host cells were part of a separate clade (Fig. 5 and S1 clade I). An exception is *L. danilewskyi*, in which the gametocytes develop both roundish and fusiform host cells. Meanwhile, parasites that produce gametocytes in fusiform cells are part of a separate monophyletic group (identified as clade II). Within this, lineages Genbank No. MK103894 of *L. neotroplcalis* and Genbank No. MK103895 of *L. grallariae* samples form a clade that is the sister lineage to *L.*

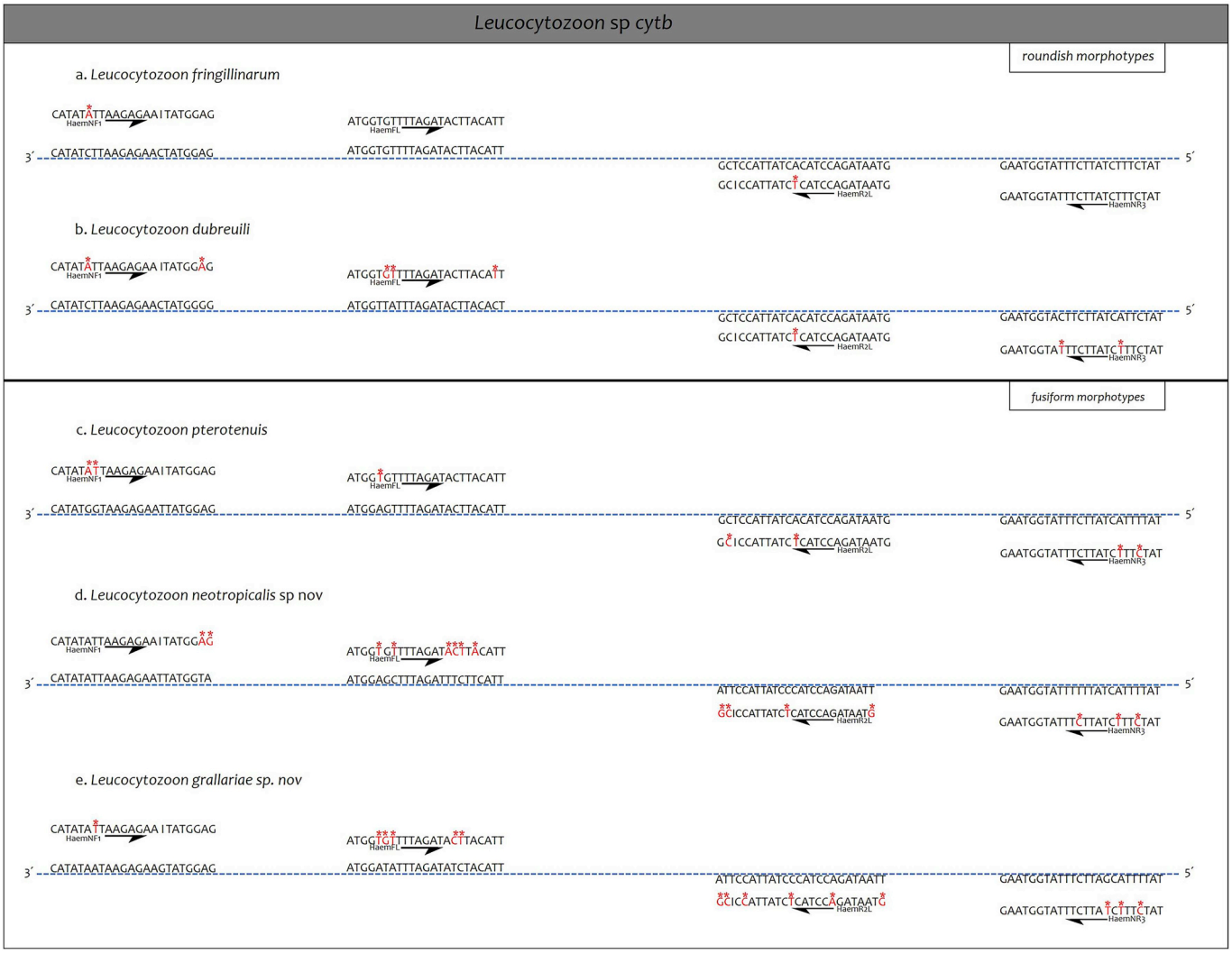

Fig. 4. Primer affinity analyses of the primers suggested by Hellgren et al. (2004). Parasites with gametocytes developing roundish host cells are: (a) *L. fringillinarum*, and (b) *L. dubreuili*; and parasites with fusiform host cell are (c) *L. pterotenuis* (in part), (d) *L. neotropicalis* sp. nov, and (e) *L. grallariae* sp. nov. An asterisk over the base pair highlights mismatches between the sequences and the primers. Note that primers HaemNR3 and HaemR2L are presented in 3′-5′ sense to fit the parasite sequences.

pterotenuis (in part) (KM272250) and *Leucocytozoon* sp. (KM272251). These parasites are closely related to *L. sabrazesi* (a morphological synonym of *Leucocytozoon macleani*, AB299369), a parasite infecting Galliformes birds, in whose gametocytes develop in fusiform host cells (Fig. 5A, Table 4). Thus, the phylogenetic analyses suggested a link between the parasite morphotypes and their sequences for both samples with co-infection.

It is worth noting that, since parasite mitochondrial genomes (mtDNA) corresponding to the partial *cytb* fragments of the MH909275 and MH909276 sequences could not be amplified, they were not included in the phylogenetic hypothesis constructed with mtDNA (Fig. 5A).

Interestingly, in clade I, the partial *cytb* lineages MH909275, MH909276 and KY646032 obtained from samples of *L. neotropicalis, L. grallariae* and *L. pterotenuis* (in part) respectively using the primers proposed by Hellgren et al. (2004) share a recent common ancestor with *L. fringillinarum* and *L. quynzae* (Fig. 5B and S1). This suggests that these lineages likely correspond to the roundish host cell morphotype coexisting with the fusiform host cell morphospecies present in the samples infected with *L. neotropicalis, L. grallariae* and *L. pterotenuis* (in part). On the other hand, *cytb* fragments obtained from mtDNA genome lineages KM272250, MK103894 and MK103895 form a monophyletic group (Fig. 5B clade II) that is a sister clade of parasites developing roundish host cells plus *L. sabrazesi* (synonym of *Leucocytozoon macleani*) (AB299369) and *L. danilewskyi* (KY653781) (Fig. 5B clade II). Both *Leucocytozoon sabrazesi* and *L. danilewskyi* are parasites with gametocytes that develop both roundish and fusiform host cells.

Phylogenetic relationships of parasite lineages with sequences isolated from South American birds are depicted in Supplementary Figure S1 (see also Supplementary Table S1). It is noteworthy that the *cytb* lineage L_GRSQU 02 (Genbank No. MH909275) obtained by PCR from the sample infected with *L. grallariae* was placed in a well-supported clade along with the lineage KY646032 isolated from the type material of *L. pterotenuis* (in part) (Fig. S1, clade E). Within the clade E, a partial *cytb* sequence of *L. quynzae* and the lineage KF874769 obtained from a Peruvian *Grallaria erythroleuca* specimen were included. Genetic distances between the isolate L_GRSQU_02 (Genbank No. MH909275) and the lineages of parasites previously reported in other species of Grallaridae (KY646032, KY646033, and KF874764) were 0.05, and 0.06 respectively; while it was 0.05 for *L. quynzae* (Fig.S1, Table 5). Furthermore, the linage L_PIRIE 02 (Genbank No. MH909276) fell into a clade composed by parasites infecting other species of *Pipreola* (Fig. S1, Clade IB). Genetic distances between this lineage and the Peruvian lineages isolated from *Pipreola* (*P.*) *intermedia* (Genbank accession No.

KF874740, KF874814) and *Pipreola arcuata* (Genbank accession Nos. KF874701, KF874796) ranged between 0,01 and 0.03 (clade B).

Consistently with phylogenetic reconstructions performed with mtDNA genome, lineages MK103895 and MK103894 fell into a clade that included *L. sabrazesi* and *L. pterotenuis* (in part) (Fig. 5A, clade II). The genetic distance between the mtDNA genome lineage MK103894 of *L. neotropicalis* and its sister taxa (KM272250) was 0.25, while the genetic distance of lineage MK103895 *L. sabrazesi*, *L. pterotenuis* (in part) and MK103894 were 0.21, 0.17, and 0.25 respectively. The large genetic distances estimated using both the partial mtDNA and the *cytb* sequences obtained from the new species as well as *L. pterotenuis* (in part) using the methodologies above mentioned are reported in Table 5.

4. Discussion

The combined use of information obtained from morphological and molecular characterizations provided opportunities to distinguish and describe two new parasite species *L. neotropicalis* and *L. grallariae*. Gametocytes of both species develop fusiform host cells that are quite scarce in the Neotropic leucocytozoids (Lotta et al., 2016, 2015) and are rare in leucocytozoids parasitizing Passeriformes birds (Valkiūnas, 2005). Nevertheless, the standard PCR protocols used to diagnose and characterize the leucocytozooids (i.e. Bensch et al., 2000; Hellgren et al., 2004; Perkins and Schall, 2002) likely underestimate the *Leucocytozoon* diversity. The mispriming found in this study explain how such protocols failed to detect parasite lineages that, in this case, seem to be endemic from the Neotropical region. Besides other factors that cause a sub-estimate of *Leucocytozoon* parasite prevalence and diversity are the sampling bias of avian hosts (most of them belong to orders Passeriformes or Apodiformes), as well as that some studies rely solely on molecular methods and did not use microscopic examination for the parasite detection (i.e., Galen and Witt, 2014; Harrigan et al., 2014).

4.1. Prevalence of Leucocytozoon parasites

In the Neotropics, the overall percentage of naturally infected birds with *Leucocytozoon* parasite is generally low (e.g., Harrigan et al., 2014; Lotta et al., 2016; Fecchio et al., 2018). Indeed, the above-cited studies report 0.06%, 1.16%, 4.6% respectively. The percentage found in this study used microscopy solely so chronical non-patent infections could be overlooked by this methodology. However, the percentage obtained (1.2%) was similar to the ones reported in the two studies mentioned above, where molecular detection of all samples was performed. However, this value is lower when it was compared with other prevalence data obtained in other zoogeographical regions (e.g. 16.2% in the Holarctic region, see Valkiūnas, 2005). New molecular protocols together with microscopy may change our perspective of how frequently these parasites are found in the neotropics. In the avian species studied in Colombia, there is marked variation in the frequency of *Leucocytozoon* parasites' found across different families. For example, all Grallariidae species studied so far are infected (100%), followed by Thraupidae (29.2%), Emberizidae (19.4%) and Turdidae (7.9%) (Lotta et al., 2016).

In this study, 4 out of 4 examined grallariids were infected. Although the sample size is small, we can speculate that these birds are highly susceptible to *Leucocytozoon* infection. Indeed, different *Leucocytozoon* species were found in these birds even in sympatric transmission, as is the case of *L. pterotenuis* (in part) in *Grallaria ruficapilla* described by (Lotta et al., 2015) and *L. grallariae* (*Grallaria squamigera*) which showed high genetic diversity (Table 5) and distinct morphological differences (Figs. 1 and 2; see also Fig. 1 in Lotta et al., 2015). An ecological aspect that can drive this feature is the preference of these birds to inhabit areas and build their nest near streams and small brooks (Stiles and López, 1995; Londoño et al., 2004), being them a readily available blood source for simuliids, their parasite vectors. Simuliids also have preferences for running and clean waters (Coscarón and Coscarón-Arias, 2007).

4.2. Analysis of primer affinities

With the affinity analysis of the primers proposed by Hellgren et al. (2004) (Fig. 4), we determine that those primers can amplify *Leucocytozoon* parasites with gametocytes that developed round host cells, like *L. fringillinarum* and *L. dubreuili*. Also, different studies have proved their efficiency in the detection of other leucocytozoids with gametocytes in fusiform host cells, such as *L. buteonis* (Krone et al., 2008), *L. danilewskyi* (Ortego and Cordero, 2009), and *L simondi* (Smith and Ramey, 2015). However, these primers did not match properly with the *cytb* sequences of *L. pterotenuis, L. grallariae*, and *L. neotropicalis*; which gametocytes develop in fusiform host cells recently described in the Neotropics. One possible explanation for these results may be due to the design of the Hellgren et al. (2004) primers, particularly the primer HaemR2L, since only the *cytb* sequences of *L. dubreuili* and *L. simondi* were available at that time (Perkins and Schall, 2002).

It is worth mentioning that despite of microscopic report of two different morphologies of *Leucocytozoon* parasites in blood films of type samples of *L. neotropicalis, L. grallariae* and *L. pterotenuis* (in part, previously described by Lotta et al., 2015), the presence of co-infections were confirmed only when molecular analyses (partial *cytb* and mitochondrial DNA genome amplification) were performed in parallel.

None of the partial *cytb* lineages obtained by mtDNA amplification could be amplified using the primers and protocols suggested by Hellgren et al. (2004). That calls for the development of a new set of primer for nested PCR-based methods diagnosis of avian leucocytozoids. The new mtDNA genomes sequences obtained in this and previous studies conducted in the Neotropics (i.e., Matta et al., 2014; Lotta et al., 2016; Pacheco et al., 2018b) and now available in public databases can be helpful for the design of a new set of primer and PCR protocols.

4.3. Diversity of Leucocytozoon lineages and primers used

Two different parasite lineages were amplified in each sample where a new parasite species was described, and that was consistent with microscopic examination. The genetic distances between the *cytb* fragments obtained by direct sequencing of the PCR product and the cloned mitochondrial lineages ranged from 0.20 to 0.29 (Table 5), indicating that two different species were co-infecting each sample. Similar to this, after the publication of *L. pterotenuis* (in part, Lotta et al., 2015), the authors found that *cytb* lineages isolated from *Grallaria ruficapilla* and *Grallaria quitensis* (obtained using the Hellgren's protocol, Hellgren et al., 2004) and used for the reconstruction of phylogenetic relationships were different from those obtained using the protocol for the parasite mtDNA genome amplification. Nevertheless, both sets of lineages - partial mtDNA genomes (GenBank accession numbers KM610045 and KM610046) and partial *cytb* genes (GenBank accession numbers KY646032 and KY646033) are true lineages. The last one we presume belongs to a morphotype also present in co-infection with *L. pterotenuis* (in part, Lotta et al., 2015).

The presence of parasites with gametocytes developing fusiform and roundish host cells in the smears does not always implicate a co-infection. Indeed, Desser (1967) proved that *Leucocytozoon simondi* has gametocytes that develop both roundish and fusiform host cells depending on the stage of exo-erythrocytic development. Mainly, merozoites from the hepatic meronts and megalomeronts produced gametocytes that develop in roundish and fusiform host cells, respectively. Nevertheless, in all our phylogenetic reconstructions, partial *cytb* fragments fell into a different clade to those *cytb* sequences derived from the mtDNA sequences. Furthermore, the microscopic examination revealed that fusiform host cells were more often seen than roundish ones in all the three samples where we have found new *Leucocytozoon* species. For example, in *G. ruficapilla,* parasitemia of *L. pteroteunuis* gametocytes in

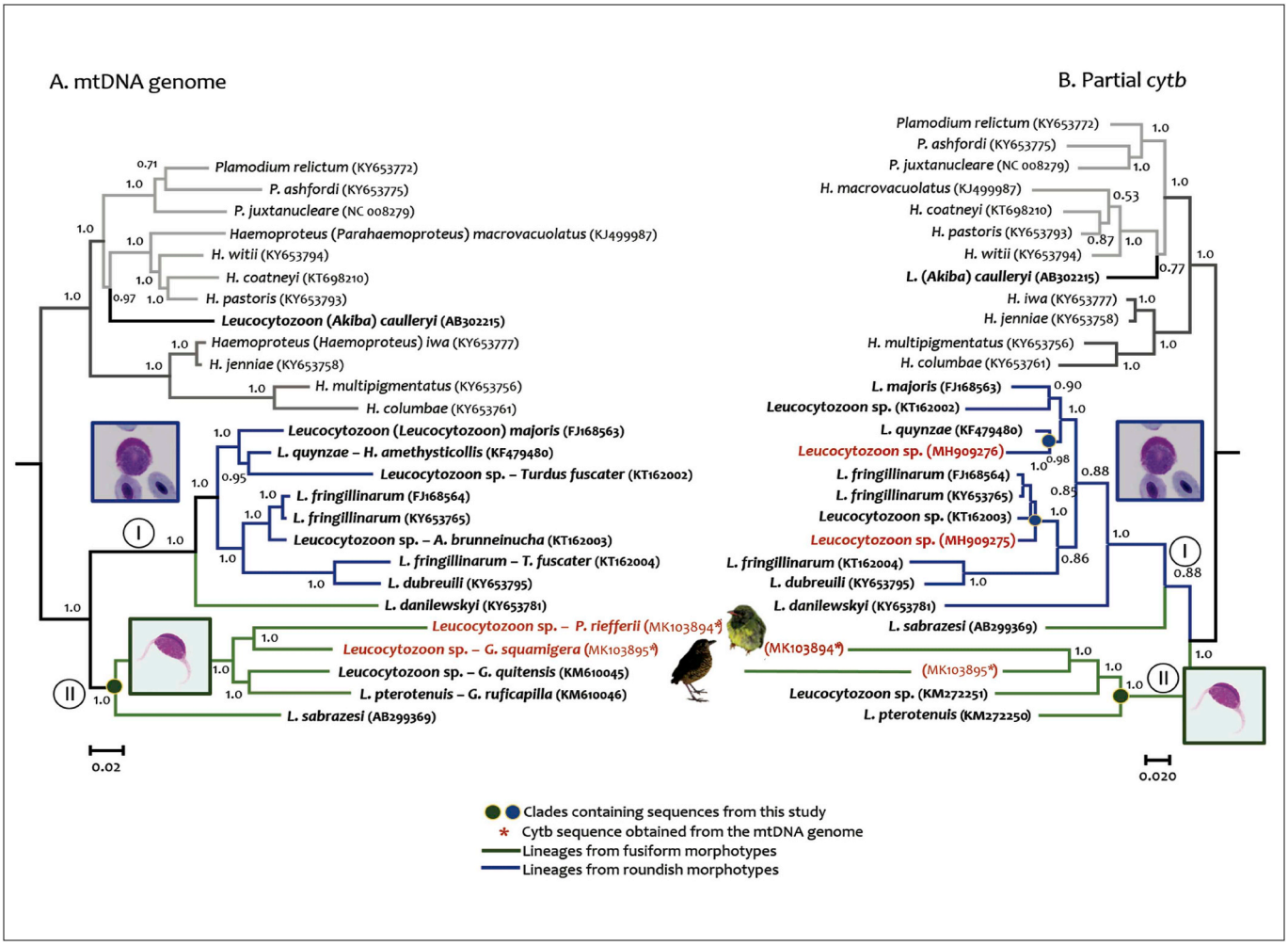

Fig. 5. (A) A Bayesian phylogenetic hypothesis of *Leucocytozoon* species constructed only with partial mitochondrial genomes (5485 bp excluding gaps) and (B) partial *cytb* gene sequences of leucocytozoids. Branch colors indicate the parasite morphology, with green branches representing parasites in fusiform host cells, and blue branches correspond to a species that develops in roundish host cells. Notice that, since parasite mitochondrial genomes (mtDNA) corresponding to the partial *cytb* fragments of the MH909275 and MH909276 sequences could not be amplified, they were not included in the phylogenetic hypothesis constructed with mtDNA (Fig. 5A). (For interpretation of the references to color in this figure legend, the reader is referred to the Web version of this article.)

Table 4
Genetic distance (d) and standard errors (SE) between pairs of species using *cox1*,*cox3*, *cytb* and mitochondrial genomes (mtDNA) sequences of *Leucocytozoon* lineages (Fig. 5).

	Genetic distance (d ± SE)			
	cox1	cox3	cytb	mitochondrial genome
L. neotropicalis[a] vs. *L. grallariae*[b]	0.090 ± 0.007	0.105 ± 0.011	0.129 ± 0.007	0.095 ± 0.004
L. neotropicalis vs. *L. pterotenuis*[c]	0.103 ± 0.008	0.116 ± 0.011	0.141 ± 0.007	0.108 ± 0.004
L. grallariae vs. *L. pterotenuis*	0.095 ± 0.007	0.119 ± 0.011	0.080 ± 0.006	0.082 ± 0.004
L. neotropicalis vs. *L. sabrazesi*	0.156 ± 0.010	0.169 ± 0.013	0.176 ± 0.006	0.149 ± 0.005
L. grallariae vs. *L. sabrazesi*	0.095 ± 0.009	0.188 ± 0.014	0.136 ± 0.006	0.131 ± 0.005
L. quynzae vs. *L. neotropicalis*	0.160 ± 0.009	0.161 ± 0.012	0.141 ± 0.008	0.146 ± 0.005
L. quynzae vs. *L. grallariae*	0.167 ± 0.010	0.181 ± 0.014	0.080 ± 0.007	0.133 ± 0.005
L. fringillinarum vs. *L. neotropicalis*	0.171 ± 0.009	0.178 ± 0.013	0.175 ± 0.007	0.150 ± 0.004
L. fringillinarum vs. *L. grallariae*	0.176 ± 0.010	0.192 ± 0.014	0.140 ± 0.007	0.139 ± 0.005
L. majoris vs. *L. fringillinarum*	0.089 ± 0.007	0.099 ± 0.011	0.048 ± 0.004	0.058 ± 0.004

Lineages amplified and cloned from.
[a] *P. riefferii* infected with *L. neotropicalis,* (GenBank MK103894).
[b] *G. squamigera* infected with *L. grallariae* (GenBank MK103895), and.
[c] *G. ruficapilla* infected with *L. pterotenuis* (Lotta et al., 2015 (partim)) (GenBank KM610046).

fusiform host cells and roundish host cells was 0.06% and 0.01%, respectively (Lotta et al., 2015). The same pattern was found in the birds infected with *L. grallariae* and *L. neotropicalis* (see above in the description remarks). The parasitemia and aforementioned analyses of primers suggest that DNA fragments of parasites from gametocytes in roundish host cells more likely were amplified by the Hellgren et al.

Table 5
Genetic distance between cytochrome b lineages of *Leucocytozoon* spp. shown in FigS1. Calculations were made using Kimura two-parameter model of substitutions.

		1	2	3	4	5	6	7	8	9	10	11	12	13	14	15	16	17	18	19	20	21	22	23	24	25
1	AB299369																									
2	JQ988502PERU	0,19																								
3	JQ988749PERU	0,18	0,23																							
4	JQ988751PERU	0,18	0,03	0,22																						
5	KF479480	0,17	0,09	0,19	0,08																					
6	KF874701PERU	0,18	0,05	0,22	0,04	0,09																				
7	KF874740PERU	0,18	0,05	0,23	0,03	0,11	0,02																			
8	KF874751PERU	0,18	0,10	0,21	0,09	0,07	0,09	0,10																		
9	KF874796PERU	0,18	0,04	0,22	0,04	0,10	0,02	0,03	0,09																	
10	KF874797PERU	0,16	0,05	0,21	0,04	0,08	0,02	0,02	0,07	0,02																
11	KF874801PERU	0,17	0,07	0,22	0,06	0,09	0,07	0,06	0,10	0,06	0,06															
12	KF874814PERU	0,17	0,05	0,21	0,04	0,08	0,03	0,03	0,07	0,03	0,01	0,06														
13	KM272250COL	0,18	0,24	0,05	0,23	0,21	0,22	0,23	0,23	0,23	0,21	0,22	0,21													
14	KM272251COL	0,23	0,21	0,15	0,21	0,22	0,20	0,21	0,22	0,21	0,20	0,24	0,20	0,17												
15	KT247892COL	0,17	0,09	0,22	0,08	0,12	0,08	0,09	0,14	0,09	0,08	0,10	0,09	0,23	0,22											
16	KY646032COL	0,18	0,10	0,19	0,10	0,05	0,10	0,11	0,08	0,10	0,08	0,10	0,08	0,20	0,24	0,12										
17	KY646033COL	0,18	0,09	0,19	0,09	0,04	0,10	0,10	0,07	0,10	0,08	0,10	0,08	0,21	0,23	0,12	0,04									
18	MG714923BRAZIL	0,18	0,12	0,23	0,11	0,08	0,10	0,11	0,07	0,11	0,08	0,10	0,09	0,23	0,26	0,13	0,10	0,08								
19	NC_012450	0,19	0,09	0,23	0,09	0,07	0,09	0,10	0,08	0,09	0,08	0,10	0,08	0,23	0,23	0,11	0,08	0,08	0,08							
20	NC_012451	0,18	0,04	0,23	0,03	0,09	0,04	0,03	0,09	0,03	0,03	0,06	0,04	0,23	0,21	0,08	0,10	0,09	0,11	0,09						
21	**MK103895**	**0,21**	**0,24**	**0,15**	**0,24**	**0,22**	**0,26**	**0,27**	**0,24**	**0,25**	**0,24**	**0,26**	**0,24**	**0,17**	**0,18**	**0,23**	**0,22**	**0,22**	**0,25**	**0,24**	**0,24**					
22	**MK103894**	**0,31**	**0,30**	**0,24**	**0,29**	**0,30**	**0,30**	**0,32**	**0,28**	**0,30**	**0,29**	**0,30**	**0,30**	**0,26**	**0,25**	**0,27**	**0,30**	**0,29**	**0,29**	**0,30**	**0,30**	**0,25**				
23	**MH909276**	**0,19**	**0,04**	**0,22**	**0,02**	**0,10**	**0,02**	**0,01**	**0,10**	**0,02**	**0,03**	**0,06**	**0,03**	**0,23**	**0,21**	**0,08**	**0,11**	**0,09**	**0,11**	**0,09**	**0,03**	**0,25**	**0,30**			
24	**MH909275**	**0,18**	**0,10**	**0,19**	**0,09**	**0,06**	**0,10**	**0,10**	**0,07**	**0,10**	**0,09**	**0,10**	**0,09**	**0,22**	**0,24**	**0,14**	**0,06**	**0,05**	**0,08**	**0,08**	**0,10**	**0,23**	**0,28**	**0,10**		
25	*FJ168562*	*0,21*	*0,22*	*0,27*	*0,22*	*0,21*	*0,22*	*0,22*	*0,23*	*0,24*	*0,22*	*0,24*	*0,22*	*0,24*	*0,29*	*0,21*	*0,23*	*0,21*	*0,24*	*0,22*	*0,22*	*0,28*	*0,32*	*0,22*	*0,22*	

Lineages obtained from the type samples of *L. gralariae* sp. nov. and *L. neotropicalis* sp. nov. are.indicated in bold. Lineage of *Haemoproteus columbae* was used as outgroup, and it is indicated in italics.

primers (Hellgren et al., 2004).

4.4. Phylogenetic relationships of parasite lineages

The association of molecular lineages and morphospecies described in this study cannot be definitively proved. However, the close relationship between the 476 bp *cytb* lineage obtained in the *L. neotropicalis* (GenBank accession No. MH909276) sample with *L. fringillinarum* (Fig. 5B, genetic distance 2.8% Table 5) suggests that the *L. neotropicalis* lineage analyzed correspond to the parasite developing in roundish host cells, which resemble *L. fringillinarum* morphological species group. On the other hand, *Leucocytozoon* parasites with gametocytes in fusiform host cells are rare in passerine birds (Lotta et al., 2015; Valkiūnas, 2005). Although *L. grallariae* lineage is part of the same clade as *L. neotropicalis* and is closely related to *L. pterotenuis* (in part), patterns of host specificity of these infections deserve more in-depth studies. It is important to mention that the *cytb* lineages obtained both for *L. grallariae* and *L. neotropicalis*, grouped with other lineages previously reported in Peru and Colombia (Lotta et al., 2016) (Fig.S1. clade B and E).

In the past decade, leucocytozoids have been the subject of intense study in the Neotropical countries (Merino et al., 2008; Rodríguez et al., 2009; Matta et al., 2014; Galen and Witt, 2014; González et al., 2014; Harrigan et al., 2014; Lotta et al., 2015, 2016). New parasite species have been described in birds with distribution limited to the Andean mountains (Matta et al., 2014; Lotta et al., 2015). Due to the bias of the bird's capture method, mainly birds of Passeriformes and Apodiformes out of the 25 bird orders present in these mountain ranges (Herzog and Kattan, 2011) have been extensively sampled. Besides, due to the high endemism and richness of host species in the Neotropics, it is possible that new host-parasite relationships and coevolution have contributed to the generation of new lineages, which are significantly different to previous ones reported in other geographical regions. We encourage researchers to perform more in-depth sampling of birds belonging to other bird orders as well as to go further in genomic studies and life cycle characterization that are helpful for estimates parasite diversity and evolutionary history of avian malaria and relative haemosporidian parasites.

Acknowledgements

We thank the students of the Host-Parasite Relationship Research Group: Avian Haemoparasites Model; especially to Paola González, for field and laboratory assistance. Also, we would like to thank the staff of Unidad Administrativa Especial del Sistema de Parques Nacionales Naturales for supporting field logistics. This study was supported by El Departamento Administrativo de Ciencias, Tecnología e Innovación COLCIENCIAS (contract No. 556–2014, project numbers 110152128340 and 110165944139), Vicerectoria de Investigación - Universidad Nacional de Colombia, project N° 38238 and Division de Investigación Bogotá-Universidad Nacional de Colombia, project N° 18714. The funding sources had no role in the study design, data collection and analysis, or preparation of the manuscript.

Appendix A. Supplementary data

Supplementary data to this article can be found online at https://doi.org/10.1016/j.ijppaw.2019.05.002.

References

Addinsoft, 2017. XLSTAT 2017: Data Analysis and Statistical Solution for Microsoft Excel. Addinsoft, Paris, France.

Bennett, G., Earlé, R., Peirce, M., Nandi, N., 1993. The Leucocytozoidae of South African birds. The coliiformes and coraciiformes. Afr. Zool. 28, 74–80. https://doi.org/10.1080/02541858.1993.11448296.

Bensch, S., Hellgren, O., Pérez-Tris, J., 2009. MalAvi: a public database of malaria parasites and related haemosporidians in avian hosts based on mitochondrial cytochrome b lineages. Mol. Ecol. Resour. 9, 1353–1358.

Bensch, S., Péarez-Tris, J., Waldenströum, J., Hellgren, O., 2004. Linkage between nuclear and mitochondrial DNA sequences in avian malaria parasites: multiple cases of cryptic speciation? Evolution 58, 1617–1621. https://doi.org/10.1111/j.0014-3820.2004.tb01742.x.

Bensch, S., Stjernman, M., Hasselquist, D., Örjan, Ö., Hannson, B., Westerdahl, H., Pinheiro, R.T., 2000. Host specificity in avian blood parasites: a study of *Plasmodium* and *Haemoproteus* mitochondrial DNA amplified from birds. Proc. R. Soc. Lond. B Biol. Sci. 267, 1583–1589.

Benson, D.A., Clark, K., Karsch-Mizrachi, I., Lipman, D.J., Ostell, J., Sayers, E.W., 2015. GenBank. Nucleic Acids Res. 43, D30–D35.

Bernotienė, R., Palinauskas, V., Iezhova, T., Murauskaitė, D., Valkiūnas, G., 2016. Avian haemosporidian parasites (Haemosporida): a comparative analysis of different polymerase chain reaction assays in detection of mixed infections. Exp. Parasitol. 163, 31–37.

BirdLife International, 2017a. Species Factsheet: *Grallaria Squamigera*. [WWW Document]. URL. http://www.birdlife.org, Accessed date: 17 September 2017.

BirdLife International, 2017b. Species Factsheet: *Pipreola Riefferii*. [WWW Document]. URL. http://www.birdlife.org, Accessed date: 17 September 2017.

Cadena-Ortiz, H., Mantilla, J.S., de Aguilar, J.R., Flores, D., Bahamonde, D., Matta, N.E., Bonaccorso, E., 2018. Avian haemosporidian infections in rufous-collared sparrows in an Andean dry forest: diversity and factors related to prevalence and parasitaemia. Parasitology 1–9.

Ciloglu, A., Ellis, V.A., Bernotienė, R., Valkiūnas, G., Bensch, S., 2018. A new one-step multiplex PCR assay for simultaneous detection and identification of avian haemosporidian parasites. Parasitol. Res. 1–11. https://doi.org/doi: 10.1007/s00436-018-6153-7.

Coscarón, S., Coscarón-Arias, C., 2007. Neotropical Simuliidae (Diptera: Simuliidae). Aquat. Biodivers. Lat. Am.

Cuatrecasas, J., 1958. Aspectos de la vegetación natural de Colombia. Rev. Acad. Colomb. Cienc. Exactas Físicas Nat. 10, 221–268.

Darriba, D., Taboada, G.L., Doallo, R., Posada, D., 2012. jModelTest 2: more models, new heuristics and parallel computing. Nat. Methods 9 772–772.

de Aguilar, J.R., Castillo, F., Moreno, A., Peñafiel, N., Browne, L., Walter, S.T., Karubian, J., Bonaccorso, E., 2018. Patterns of avian haemosporidian infections vary with time, but not habitat, in a fragmented Neotropical landscape. PLoS One 13, e0206493.

Desser, S., 1967. Schizogony and gametogony of *Leucocytozoon simondi* and associated reactions in the avian host. J. Eukaryot. Microbiol. 14, 244–254.

Escalante, A.A., Freeland, D.E., Collins, W.E., Lal, A.A., 1998. The evolution of primate malaria parasites based on the gene encoding *cytochrome b* from the linear mitochondrial genome. Proc. Natl. Acad. Sci. Unit. States Am. 95, 8124–8129. https://doi.org/10.1073/pnas.95.14.8124.

Fecchio, A., Silveira, P., Weckstein, J., Dispoto, J., Anciães, M., Bosholn, M., Tkach, V., Bell, J., 2018. First record of *Leucocytozoon* (Haemosporida: Leucocytozoidae) in Amazonia: evidence for rarity in Neotropical lowlands or lack of sampling for this parasite genus? J. Parasitol. 104, 168–172.

Galen, S.C., Witt, C.C., 2014. Diverse avian malaria and other haemosporidian parasites in Andean house wrens: evidence for regional co-diversification by host-switching. J. Avian Biol. 45, 374–386.

Gil-Vargas, D.L., Sedano-Cruz, R.E., 2019. Genetic variation of avian malaria in the tropical Andes: a relationship with the spatial distribution of hosts. Malar. J. 18, 129.

González, A.D., Lotta, I.A., García, L.F., Moncada, L.I., Matta, N.E., 2015. Avian haemosporidians from Neotropical highlands: evidence from morphological and molecular data. Parasitol. Int. 64, 48–59.

González, A.D., Matta, N.E., Ellis, V.A., Miller, E.T., Ricklefs, R.E., Gutiérrez, H.R., 2014. Mixed species flock, nest height, and elevation partially explain avian haemoparasite prevalence in Colombia. PLoS One 9, e100695.

Greiner, E.C., 1976. *Leucocytozoon maccluri* sp. n. (Haemosporida: Leucocytozoidae) from a Thailand thrush, *Zoothera marginata* Blyth. J. Parasitol. 62, 545–547. https://doi.org/10.2307/3279409.

Harrigan, R.J., Sedano, R., Chasar, A.C., Chaves, J.A., Nguyen, J.T., Whitaker, A., Smith, T.B., 2014. New host and lineage diversity of avian haemosporidia in the northern Andes. Evol. Appl. 7, 799–811.

Hellgren, O., Waldenström, J., Bensch, S., 2004. A new PCR assay for simultaneous studies of *Leucocytozoon, Plasmodium*, and *Haemoproteus* from avian blood. J. Parasitol. 90, 797–802.

Herzog, S.K., Kattan, G.H., 2011. Patterns of diversity and endemism in the birds of the tropical Andes. Clim. Change Biodivers. Trop. Andes McArthur Found. Inter-Am. Inst. Glob. Change Res. IAI Sci. Comm. Probl. Environ. SCOPE Paris 245–259.

International Commission on Zoological Nomenclature, 1999. International Code of Zoological Nomenclature, fourth ed. International Trust for Zoological Nomenclature, London.

Jones, M., Cheviron, Z., Carling, M., 2013. Spatial patterns of avian malaria prevalence in *Zonotrichia capensis* on the western slope of the Peruvian Andes. J. Parasitol. 99, 903–906.

Josse, C., Cuesta, F., Navarro, G., Barrena, V., Cabrera, E., Chacón-Moreno, E., Ferreira, W., Peralvo, M., Saito, J., Tovar, A., 2009. Ecosistemas de los Andes del norte y centro. Bolivia, Colombia, Ecuador, Perú y Venezuela. Secr. Gen. Comunidad Andina Lima.

Krone, O., Waldenström, J., Valkiūnas, G., Lessow, O., Müller, K., Iezhova, T.A., Fickel, J., Bensch, S., 2008. Haemosporidian blood parasites in European birds of prey and owls. J. Parasitol. 94, 709. https://doi.org/10.1645/GE-1357R1.1.

Kumar, S., Stecher, G., Tamura, K., 2016. MEGA7: molecular evolutionary genetics analysis version 7.0 for bigger datasets. Mol. Biol. Evol. 33, 1870–1874.

Londoño, G.A., Saavedra-R, C.A., Osorio, D., Martínez, J., 2004. Notas sobre la anidación

del Tororoi Bigotudo (*Grallaria alleni*) en la Cordillera Central de Colombia. Ornitol. Colomb. 2, 19–24.
Lotta, I.A., Gonzalez, A.D., Pacheco, M.A., Escalante, A.A., Valkiūnas, G., Moncada, L.I., Matta, N.E., 2015. *Leucocytozoon pterotenuis* sp. nov.(Haemosporida, Leucocytozoidae): description of the morphologically unique species from the Grallariidae birds, with remarks on the distribution of *Leucocytozoon* parasites in the Neotropics. Parasitol. Res. 114, 1031–1044.
Lotta, I.A., Pacheco, M.A., Escalante, A.A., González, A.D., Mantilla, J.S., Moncada, L.I., Adler, P.H., Matta, N.E., 2016. *Leucocytozoon* diversity and possible vectors in the neotropical highlands of Colombia. Protist 167, 185–204.
Mantilla, J.S., González, A.D., Lotta, I.A., Moens, M., Pacheco, M.A., Escalante, A.A., Valkiūnas, G., Moncada, L.I., Pérez-Tris, J., Matta, N.E., 2016. *Haemoproteus erythrogravidus* n. sp.(Haemosporida, Haemoproteidae): description and molecular characterization of a widespread blood parasite of birds in South America. Acta Trop. 159, 83–94.
Mantilla, J.S., González, A.D., Valkiūnas, G., Moncada, L.I., Matta, N.E., 2013. Description and molecular characterization of Plasmodium (Novyella) unalis sp. nov. from the Great Thrush (Turdus fuscater) in highland of Colombia. Parasitol. Res. 112, 4193–4204.
Martinsen, E.S., Perkins, S.L., Schall, J.J., 2008. A three-genome phylogeny of malaria parasites (*Plasmodium* and closely related genera): evolution of life-history traits and host switches. Mol. Phylogenetics Evol. 47, 261–273.
Marzal, A., García-Longoria, L., Cárdenas Callirgos, J., Sehgal, R., 2015. Invasive avian malaria as an emerging parasitic disease in native birds of Peru. Biol. Invasions 17, 39–45. https://doi.org/10.1007/s10530-014-0718-x.
Matta, N.E., Lotta, I.A., Valkiūnas, G., González, A.D., Pacheco, M.A., Escalante, A.A., Moncada, L.I., Rodríguez-Fandiño, O.A., 2014. Description of *Leucocytozoon quynzae* sp. nov.(Haemosporida, Leucocytozoidae) from hummingbirds, with remarks on distribution and possible vectors of leucocytozoids in South America. Parasitol. Res. 113, 457–468.
McMullan, M., Quevedo, A., Donegan, T.M., 2011. Guía de campo de las aves de Colombia. ProAves.
McWilliam, H., Li, W., Uludag, M., Squizzato, S., Park, Y.M., Buso, N., Cowley, A.P., Lopez, R., 2013. Analysis tool web services from the EMBL-EBI. Nucleic Acids Res. 41, W597–W600.
Merino, S., Moreno, J., Vásquez, R.A., Martinez, J., Sanchez-Monsalvez, I., Estades, C.F., Ippi, S., Sabat, P., Rozzi, R., Mcgehee, S., 2008. Haematozoa in forest birds from southern Chile: latitudinal gradients in prevalence and parasite lineage richness. Austral Ecol. 33, 329–340.
Miller, M.A., Pfeiffer, W., Schwartz, T., 2010. Creating the CIPRES Science Gateway for inference of large phylogenetic trees. In: Gateway Computing Environments Workshop. GCE), Ieee, pp. 1–8 2010.
Moens, M.A., Pérez-Tris, J., 2016. Discovering potential sources of emerging pathogens: South America is a reservoir of generalist avian blood parasites. Int. J. Parasitol. 46, 41–49.
Moens, M.A., Valkiūnas, G., Paca, A., Bonaccorso, E., Aguirre, N., Pérez-Tris, J., 2016. Parasite specialization in a unique habitat: hummingbirds as reservoirs of generalist blood parasites of Andean birds. J. Anim. Ecol. 85, 1234–1245.
Morrone, J.J., 2001. Biogeografía de América Latina y el Caribe, first ed. M&T – Manuales y Tesis SEA, Zaragoza, España.
Muñoz, E., Ferrer, D., Molina, R., Adlard, R., 1999. Prevalence of haematozoa in birds of prey in Catalonia, north-east Spain. Vet. Rec. 144, 632–636.
Myers, N., Mittermeier, R.A., Mittermeier, C.G., Da Fonseca, G.A., Kent, J., 2000. Biodiversity hotspots for conservation priorities. Nature 403, 853.
Ortego, J., Cordero, P.J., 2009. PCR-based detection and genotyping of haematozoa (Protozoa) parasitizing eagle owls, *Bubo bubo*. Parasitol. Res. 104, 467–470. https://doi.org/10.1007/s00436-008-1207-x.
Pacheco, M.A., Battistuzzi, F.U., Junge, R.E., Cornejo, O.E., Williams, C.V., Landau, I., Rabetafika, L., Snounou, G., Jones-Engel, L., Escalante, A.A., 2011. Timing the origin of human malarias: the lemur puzzle. BMC Evol. Biol. 11, 299.
Pacheco, M.A., Cepeda, A.S., Bernotienė, R., Lotta, I.A., Matta, N.E., Valkiūnas, G., Escalante, A.A., 2018a. Primers targeting mitochondrial genes of avian haemosporidians: PCR detection and differential DNA amplification of parasites belonging to different genera. Int. J. Parasitol.
Pacheco, M.A., Matta, N.E., Valkiūnas, G., Parker, P.G., Mello, B., Stanley, C.E., Lentino, M., Garcia-Amado, M.A., Cranfield, M., Kosakovsky Pond, S.L., 2018b. Mode and rate of evolution of haemosporidian mitochondrial genomes: timing the radiation of avian parasites. Mol. Biol. Evol. 35, 383–403. https://doi.org/10.1093/molbev/msx285.
Peirce, M.A., 1984. Haematozoa of Zambian birds. IV. Description of *Leucocytozoon balmorali* sp. nov. from Malaconotidae. J. Nat. Hist. 18, 223–226. https://doi.org/10.1080/00222938400770181.
Perez-Tris, J., Bensch, S., 2005. Diagnosing genetically diverse avian malarial infections using mixed-sequence analysis and TA-cloning. Parasitology 131, 15–23.
Perkins, S.L., 2008. Molecular systematics of the three mitochondrial protein-coding genes of malaria parasites: corroborative and new evidence for the origins of human malaria. DNA Seq 19, 471–478.
Perkins, S.L., Schall, J., 2002. A molecular phylogeny of malarial parasites recovered from *cytochrome b* gene sequences. J. Parasitol. 88, 972–978.
Rambaut, A., 2006. FigTree. Tree Figure Drawing Tool Version 1.3. 1. Institute of Evolutionary biology, University of Edinburgh.
Remsen, J.V., Cadena, C., Jaramillo, A., Nores, M., Areta, J., Claramunt, S., Pacheco, J., Pérez-Emán, J., Robbins, M., Stiles, F., Stotz, D., Zimmer, K., 2012. The South American Classification Committee of the American Ornithologists' Union: a New Classification of the Birds of South America. [WWW Document]. URL. http://www.museum.lsu.edu/~Remsen/2007-NeotropicalBirding.pdf, Accessed date: 19 September 2017.
Richard, F.A., Sehgal, R.N., Jones, H.I., Smith, T.B., 2002. A comparative analysis of PCR-based detection methods for avian malaria. J. Parasitol. 88, 819–822.
Rodríguez, O.A., Moya, H., Matta, N.E., 2009. Avian blood parasites in the National natural Park Chingaza: high Andes of Colombia. Hornero 24, 1–6.
Ronquist, F., Huelsenbeck, J.P., 2003. MrBayes 3: Bayesian phylogenetic inference under mixed models. Bioinformatics 19, 1572–1574.
Sambrook, J., Fritsch, E.F., Maniathis, T., 1989. Molecular Cloning, 2nd Cold Spring Harbor. Lab Press, NY USA.
Schaer, J., Reeder, D.M., Vodzak, M.E., Olival, K.J., Weber, N., Mayer, F., Matuschewski, K., Perkins, S.L., 2015. *Nycteria* parasites of Afrotropical insectivorous bats. Int. J. Parasitol. 45, 375–384.
Schneider, C.A., Rasband, W.S., Eliceiri, K.W., 2012. NIH Image to ImageJ: 25 years of image analysis. Nat. Methods 9, 671–675.
Smith, M.J., Ramey, A., 2015. Prevalence and genetic diversity of haematozoa in South American waterfowl and evidence for intercontinental redistribution of parasites by migratory birds. Int. J. Parasitol. Parasites Wildl. 4, 22–28. https://doi.org/10.1016/j.ijppaw.2014.12.007.
Stiles, F., López, H.A., 1995. La situación del Tororoi pechicanela (*Grallaria haplonota*, Formicariidae) en Colombia. Caldasia 17, 607–610.
Valkiūnas, G., 2005. Avian Malaria Parasites and Other Haemosporidia. CRC Press, Boca Raton.
Valkiunas, G., Iezhova, T.A., Mironov, S.V., 2002. *Leucocytozoon hamiltoni* n. sp. (Haemosporida, Leucocytozoidae) from the Bukharan great tit *Parus bokharensis*. J. Parasitol. 88, 577. https://doi.org/10.2307/3285453.
Valkiūnas, G., Sehgal, R.N., Iezhova, T.A., Hull, A.C., 2010. Identification of *Leucocytozoon toddi* group (Haemosporida: Leucocytozoidae), with remarks on the species taxonomy of leucocytozoids. J. Parasitol. 96, 170–177.
Van Rooyen, J., Lalubin, F., Glaizot, O., Christe, P., 2013. Avian haemosporidian persistence and co-infection in great tits at the individual level. Malar. J. 12, 40.
Zehtindjiev, P., Križanauskienė, A., Bensch, S., Palinauskas, V., Asghar, M., Dimitrov, D., Scebba, S., Valkiūnas, G., 2012. A new morphologically distinct avian malaria parasite that fails detection by established polymerase chain reaction–based protocols for amplification of the *cytochrome b* gene. J. Parasitol. 98, 657–665.